Università Campus Bio-Medico di Roma

Corso di dottorato di ricerca in Scienze Biomediche Integrate e Bioetica
XXXVIII ciclo a.a. 2022-2023

Neurophysiological correlates of network dysfunction in prodromal Alzheimer's disease

Davide Norata

Coordinatore
Prof. Raffaele Antonelli Incalzi

Tutore
Prof. Vincenzo Di Lazzaro

Gennaio 2026

Table of contents

List of figures

Abstract

Alzheimer's disease (AD) is characterized by a long prodromal phase in which subtle functional alterations precede overt cognitive decline and structural neurodegeneration. Identifying sensitive markers of early network dysfunction and short-term disease progression remains a major clinical challenge.

The present doctoral thesis investigated functional neurophysiological alterations in patients with biomarker-confirmed mild cognitive impairment due to Alzheimer's disease (MCI-AD), with the aim of identifying biomarkers of early network dysfunction, prognostic stratification, and potential targets for therapeutic modulation.

Across three complementary studies, a multimodal neurophysiological approach was adopted, combining conventional and high-frequency components of somatosensory evoked potentials (SEPs), together with transcranial magnetic stimulation (TMS).

Study 1 demonstrated that MCI-AD patients exhibit marked alterations in high-frequency SEP components (HFOs) despite preserved conventional SEP parameters, suggesting early disruption of fast thalamocortical and intracortical network dynamics.
Study 2 showed that baseline prolongation of early HFO duration independently predicted short-term cognitive decline, supporting the prognostic value of SEP-derived functional markers.
Study 3 explored the effects of chronic genistein supplementation on cognitive and neurophysiological outcomes, revealing subtle, time-dependent patterns in high-frequency SEP components, consistent with modulation of network-level processes.

Taken together, the findings of this thesis support the view that SEP-derived HFOs capture early alterations in network dynamics that are clinically relevant in prodromal AD. These results highlight the potential role of advanced neurophysiological measures as functional biomarkers for risk stratification and for the evaluation of early-stage interventions targeting network dysfunction in Alzheimer's disease.

Keywords

(i) Alzheimer's disease; (ii) Somatosensory evoked potentials; (iii) High-frequency oscillations; (iv) Network dysfunction; (v) Neurophysiological biomarkers.

Neurophysiological correlates of network dysfunction in prodromal Alzheimer's disease

1. Introduction

1.1 Mild Cognitive Impairment due to Alzheimer's Disease (MCI-AD)

Alzheimer's disease (AD) is a progressive neurodegenerative disorder and the leading cause of dementia globally. Pathologically, it is defined by the accumulation of extracellular amyloid-β (Aβ) plaques and intracellular neurofibrillary tangles composed of hyperphosphorylated tau, leading to synaptic dysfunction, neuronal loss, and cognitive decline over time. These neuropathological findings first appear in neocortical regions involved in cognition—mainly the entorhinal cortex and the hippocampal formation—and later spreads to neural hubs that underlie motor and sensory structures, planning, emotion and spatial navigation (Braak and Del Tredici, 2011; Forsberg et al., 2008; Jack et al., 2010; Wong et al., 2010).

According to the Global Burden of Disease Study 2019, more than 57 million people worldwide were living with dementia in 2019, with numbers expected to rise to over 150 million by 2050 (GBD 2019 Dementia Forecasting Collaborators, 2022). In Europe, the prevalence of dementia among individuals over the age of 65 is estimated at 5–7%, with a higher incidence in women (Gustavsson et al., 2023). Social determinants—particularly educational attainment—significantly influence dementia incidence and patterns of healthcare access in aging populations, as demonstrated in a recent large-scale Italian cohort study (Cristofalo et al., 2025).

AD is currently conceptualized as a biological continuum encompassing asymptomatic preclinical stages, mild cognitive impairment (MCI), and overt dementia. MCI due to AD (MCI-AD) represents a symptomatic prodromal phase characterized by objective cognitive impairment, primarily in episodic memory, without significant loss of functional independence. Patients with MCI typically present with Mini-Mental State Examination (MMSE) scores ranging between 24 and 27 (Albert et al., 2011).

The introduction of the A/T/(N) biomarker framework has revolutionized the diagnosis of AD, enabling classification based on amyloid deposition -A, tau pathology -T, and neurodegeneration -(N) (Jack et al., 2018). An A+T+ profile confirms AD pathophysiology, even in the absence of overt clinical symptoms. The most recent diagnostic frameworks—proposed by both the National Institute on Aging e la Alzheimer's Association (NIA-AA) and the International Working Group

(IWG)—differ in their application of these biomarkers. While the NIA-AA criteria define AD biologically, allowing diagnosis in preclinical stages based on biomarker positivity alone (Jack et al., 2024), the IWG criteria require both clinical symptoms and biomarker confirmation for a diagnosis (Dubois et al., 2024).

Prognostic studies have shown that the presence of both amyloid and tau biomarkers in individuals with MCI significantly increases the risk of progression to dementia. According to a prospective study by Vos and colleagues, individuals with MCI and an A+T+ profile exhibited a 50% conversion rate to dementia within three years (Vos et al., 2013). These findings underscore the importance of identifying high-risk patients during the prodromal phase.

The recent approval of disease-modifying therapies has renewed the urgency of early and accurate diagnosis. Anti-amyloid monoclonal antibodies such as lecanemab and donanemab have shown efficacy in reducing amyloid plaque burden and slowing cognitive decline in patients with early symptomatic AD (van Dyck et al., 2023; Mintun et al., 2021). In the TRAILBLAZER-ALZ 2 trial, donanemab was particularly effective in individuals with low to intermediate tau pathology and led to a 35% reduction in the rate of clinical progression compared to placebo (Mintun et al., 2021). Similarly, the CLARITY-AD trial demonstrated that lecanemab slowed cognitive and functional decline by 27% over 18 months (van Dyck et al., 2023).

However, these therapies are not without risk. Amyloid-related imaging abnormalities (ARIA), including vasogenic edema and microhemorrhages, are among the most significant adverse effects and occur in approximately 20–30% of treated individuals, necessitating careful patient selection and regular brain magnetic resonance imaging (MRI) monitoring (Budd Haeberlein et al., 2022). Consequently, selecting appropriate candidates and optimizing dosing strategies has become a clinical priority.

In this context, identifying reliable prognostic indicators of short-term disease progression in patients with MCI due to AD is essential. Such markers may guide therapeutic decisions, particularly regarding the initiation of monoclonal antibody treatment and its optimal dosing schedule.

1.2 Neuropsychiatric symptoms and the dopaminergic hypothesis in MCI-AD patients

1.2.1 Neuropsychiatric symptoms in MCI-AD patients

Neuropsychiatric symptoms (NPS) are highly prevalent throughout the course of Alzheimer's disease, affecting up to half of individuals with MCI-AD and nearly all patients with AD dementia (Lyketsos et al., 2011; Mortby et al., 2018, 2017; Peters et al., 2015).
These symptoms include depression, anxiety, psychosis, agitation, irritability, and sleep disturbances. Among them, apathy—defined as a reduction in motivation, diminished interest, and blunted emotional responsiveness (Miller et al., 2021) —is the most frequent, with a prevalence of approximately 50% in MCI-AD and up to 80% in AD dementia patients (Lanctôt et al., 2017; Ma, 2020; Sherman et al., 2018; Zhao et al., 2016).

NPS substantially contribute to functional decline and disability, increase hospitalization rates and healthcare-related costs, and markedly exacerbate caregiver burden due to the growing dependence of patients in activities of daily living (Geda et al., 2008; van der Linde et al., 2017).
Notably, apathy has also been associated with an increased risk of mortality in both dementia patients and the elderly population (Hölttä et al., 2012; Nijsten et al., 2017).

Given their profound clinical and societal impact, interventions targeting NPS may significantly improve patient outcomes, caregiver well-being, and healthcare sustainability. In this context, a deeper understanding of the biological mechanisms underlying apathy and other NPS in AD is essential, as it may enhance disease characterization, enable earlier diagnosis, and foster the development of more effective therapeutic and care strategies.

1.2.2 The dopaminergic hypothesis: evidence from preclinical and clinical studies

The growing recognition of NPS in MCI and early AD has prompted numerous investigations employing poTst-mortem analyses, metabolic studies, and neuroimaging approaches to identify brain alterations associated with these symptoms, with particular emphasis on apathy and depression. Collectively, these studies highlight structural and functional abnormalities predominantly within the medial frontal cortex, as well as in interconnected regions such as the anterior and posterior cingulate cortex, the medial orbitofrontal cortex, and the ventral striatum (Chan et al., 2021; Le Heron et al., 2018; Mortby et al., 2022; Theleritis et al., 2014). All these regions receive direct monosynaptic dopaminergic projections from the ventral tegmental area (VTA) of the midbrain. The prominent involvement of dopamine-modulated circuits in apathy and

depression supports the notion that these symptoms may, at least in part, reflect a hypodopaminergic state (Le Heron et al., 2018; Udo et al., 2020).

The mesocorticolimbic dopaminergic system originates from dopamine neuron cell bodies located in the VTA, which send long-range ascending projections via the medial forebrain bundle to limbic and cortical regions, forming the mesolimbic and mesocortical pathways, respectively (Krashia et al., 2022).
Early post-mortem studies in AD patients reported reduced expression of dopamine receptors, the dopamine transporter (DAT), and tyrosine hydroxylase (TH)—the rate-limiting enzyme for dopamine synthesis—particularly in mesocorticolimbic target regions such as the prefrontal cortex, nucleus accumbens, and hippocampus. Moreover, approximately 40% of AD cases exhibit pathological alterations within the VTA itself, including amyloid-β plaques, neurofibrillary tangles, and reduced dopamine content (for a comprehensive review, see (Krashia et al., 2022)).

Preclinical studies in the Tg2576 mouse model of Alzheimer's disease provided direct evidence for an early involvement of dopaminergic dysfunction in AD. Tg2576 mice exhibit early synaptic and cognitive deficits that temporally correlate with selective degeneration of VTA dopaminergic neurons, reduced hippocampal dopamine release, and local neuroinflammation, while other dopaminergic nuclei remain initially spared (Cordella et al., 2018; Gloria et al., 2021; Krashia et al., 2019; Moreno-Castilla et al., 2016; Nobili et al., 2017; Vorobyov et al., 2019). Pharmacological or neuroprotective interventions targeting dopamine signalling or VTA neuron survival rescue synaptic plasticity, memory impairments, and depressive-like behaviours (Nobili et al., 2017). These findings, indicate that early mesocorticolimbic dopamine loss precedes classical AD pathology in target regions and may contribute to both cognitive deficits and neuropsychiatric symptoms, likely driven by soluble Aβ toxicity at pre-plaque stages.

Consistent with preclinical evidence from transgenic mouse models, recent human neuroimaging studies have demonstrated that the VTA and its mesocorticolimbic dopaminergic projections are affected at AD very early stages. Resting-state functional MRI studies revealed a significant functional disconnection between the VTA and key cortical and limbic regions, including the hippocampus, medial temporal areas, and components of the default-mode network, with a progressive extension of these alterations as the disease advances to dementia (Bozzali et al., 2011; Gili et al., 2011; Serra et al., 2018).

Importantly, these changes show a selective vulnerability of the mesocorticolimbic system, while the nigrostriatal pathway remains relatively preserved in the early phases of the disease. Structural and metabolic imaging further demonstrated that reductions in VTA volume, grey matter atrophy, and hypometabolism in VTA target regions are closely associated with hippocampal dysfunction, memory impairment, and the severity of neuropsychiatric symptoms. Notably, functional disconnection of the VTA has been directly linked to the early appearance of apathy, depression, and anxiety since the MCI stage, supporting a mechanistic link between dopaminergic dysfunction and neuropsychiatric manifestations of AD (Iaccarino et al., 2020; Manca et al., 2023).

Together with findings from animal models, these clinical data indicate that mesocorticolimbic dopaminergic dysfunction represents an early and relatively stable pathological event in AD progression, preceding widespread cortical degeneration and classical neuropathological hallmarks in target regions. The close association between VTA disconnection, neuropsychiatric symptoms, and accelerated conversion from MCI to AD highlights the dopaminergic system not only as a contributor to cognitive decline but also as a key modulator of disease trajectory. Altogether, these observations support the notion that early alterations of the VTA and its projections may serve as valuable biomarkers for disease prognosis and represent promising targets for therapeutic strategies aimed at neuropsychiatric symptoms in Alzheimer's disease.

1.2.3 Genistein for restoring dopaminergic transmission in mesocorticolimbic dopamine system

Phytoestrogens are plant-derived compounds that structurally and functionally resemble mammalian oestrogens. Among them, genistein is a naturally occurring flavonoid belonging to the isoflavone subclass and is one of the most extensively studied phytoestrogens. It is predominantly found in legumes, including Lupinus albus (*lupine*), Vicia faba (*fava bean*), Glycine max (*soybean*), Pueraria lobata (*kudzu*), and Psoralea corylifolia (Kaufman et al., 1997; Kim et al., 2014, 2009).

Chemically, genistein (5,7-dihydroxy-3-(4-hydroxyphenyl)chromen-4-one) has the molecular formula $C_{15}H_{10}O_5$, with a molecular weight of 270.24 g/mol. Its structure is based on a 3-phenylchromen-4-one backbone, composed of two aromatic rings (A and B) linked by a heterocyclic pyran ring (C). The molecule contains a double bond between positions 2 and 3 of ring C, a carbonyl group at position 4, and three hydroxyl groups located at positions 5 and 7 of ring A and at position 4′ of ring B (Tuli et al., 2019).

Owing to these structural and biochemical features, genistein has attracted considerable interest for its potential health-promoting properties. Several studies have reported protective effects against osteoporosis, a reduced risk of cardiovascular disease, alleviation of postmenopausal symptoms, and anticancer activity (Chen et al., 2020; Marini et al., 2007; Si and Liu, 2007; Thangavel et al., 2019).

At the molecular level, genistein binds oestrogen receptors (ERs) and activates oestrogen-responsive gene transcription, albeit with a lower affinity than oestradiol (Jørgensen et al., 2000; Miodini et al., 1999). Despite this reduced binding affinity, genistein exerts oestrogen-like effects in multiple tissues, a property that has been extensively documented (Ju et al., 2001; Markiewicz et al., 1993). In addition to its hormonal actions, displays potent antioxidant properties, efficiently scavenging aqueous-phase free radicals and thereby contributing to the reduction of oxidative stress (Ruiz-Larrea et al., 1997).

Beyond its hormonal and antioxidant actions, genistein has also been shown to modulate dopaminergic signaling. Dietary exposure to genistein enhances amphetamine-induced dopamine release in the striatum of both male and female rats, mimicking the effects of estradiol (Ferguson et al., 2002).
Consistently, in an ovariectomized MPTP-induced mouse model of Parkinson's disease, genistein administration initiated prior to and maintained throughout toxin exposure significantly attenuated nigrostriatal neurodegeneration. Genistein preserved striatal dopamine levels and its metabolites, maintained tyrosine hydroxylase–immunoreactive neurons in the substantia nigra pars compacta, and restored MPTP-induced reductions in tyrosine hydroxylase and dopamine transporter mRNA expression in the midbrain, indicating a robust neuroprotective effect on dopaminergic function (Liu et al., 2008).

Importantly, evidence from both experimental and clinical studies suggests that dietary soy phytoestrogens, including genistein, exert beneficial effects on cognitive function. Improvements in working, short-term, and long-term memory have been reported in ovariectomized rodents as well as in healthy human subjects following soy-rich diets (File et al., 2001; Pan et al., 2000). Moreover, in a rat model of Alzheimer's disease based on amyloid-$\beta_{(1–40)}$ administration, genistein pretreatment attenuated Aβ-induced impairments in short-term spatial memory through estrogen receptor–dependent mechanisms and a reduction of oxidative stress (Bagheri et al., 2011).

Taken together, these findings indicate that genistein exerts combined estrogenic, antioxidant, dopaminergic, and cognitive-protective effects, supporting the hypothesis that genistein-based interventions may represent a promising therapeutic strategy for patients with Alzheimer's disease at early stages, when neuroprotective mechanisms are still accessible.

1.3 Neurophysiological assessment in Alzheimer's Disease

Neurophysiology offers a valuable approach to investigate the functional alterations associated with AD, especially during its prodromal stages, providing tools to explore the pathophysiological mechanisms that characterize both the early phases and the progression of the disease. Techniques such as standard or quantitative electroencephalography (EEG or qEEG), transcranial magnetic stimulation (TMS), and somatosensory evoked potentials (SEPs) offer non-invasive, real-time insights into cortical excitability, synaptic integrity, and network-level dysfunction.

In particular, EEG studies highlight alterations in cortical oscillatory activity characterized by a reduction in alpha and beta band power and a parallel increase in delta and theta activity. Those patterns correlate with the disease severity and synaptic degeneration (Babiloni et al., 2014; Moretti, 2015). Furthermore, qEEG analysis refines these observations by quantifying spectral ratios such as theta/gamma and alpha3/alpha2. These ratios reflect changes in brain network dynamics, as an increased theta/gamma ratio may indicate reduced cognitive efficiency, while a higher alpha3/alpha2 ratio has been associated with early dysfunction in temporo-parietal areas. Both markers have shown high sensitivity in distinguishing individuals with MCI who will convert to Alzheimer's disease from those who will not, and in tracking disease progression (Moretti, 2015). The electrophysiological changes reflect the disruptions in functional connectivity that characterize AD as a "synaptopathy", a term representing the damage and loss of synapses as the disease progresses (Kerrigan and Randall, 2013).

TMS parameters like short-latency afferent inhibition (SAI) and short-interval intracortical inhibition (SICI) have demonstrated impaired cortical inhibition and increased excitability in AD patients, reflecting cholinergic and GABAergic deficits, respectively (Di Lazzaro et al., 2004).

Conventional SEP components and high-frequency SEP components (HFOs) provide additional markers of thalamo-cortical and cortico-cortical transmission integrity (Ozaki and Hashimoto, 2011).

Overall, neurophysiological tools broaden our ability to characterize Alzheimer's Disease-related dysfunctions beyond structural imaging and molecular biomarkers, offering dynamic, low-cost, and repeatable approach for early diagnosis and monitoring.
The adoption of robust and cost-effective tools for prognostic stratification is of paramount importance for improving clinical outcomes and managing the growing AD burden effectively. Moreover, with the recent approval of anti-amyloid monoclonal antibodies, there is a renewed emphasis on identifying patients with MCI due to AD who are most likely to benefit from early intervention.
In this context, neurophysiological biomarkers may serve as sensitive indicators of short-term disease progression and help personalize treatment strategies.
Furthermore, because techniques like TMS and SEP are repeatable, non-invasive and relatively cost-effective, they represent a promising tool for monitoring of neuronal function in real-life clinical settings (Rossini and Rossi, 2007).

1.4 General aims

The general aim of this doctoral thesis was to investigate functional neurophysiological alterations associated with prodromal Alzheimer's disease, with the objective of identifying sensitive biomarkers of early network dysfunction and short-term disease progression. To this end, the thesis adopted a multimodal neurophysiological approach to characterize alterations in cortical and thalamocortical function in patients with mild cognitive impairment due to Alzheimer's disease. In addition, this work explored whether selected neurophysiological measures could capture longitudinal changes over time and provide complementary information to established molecular biomarkers. Finally, the thesis examined the effects of a pharmacological intervention on cognitive performance and neurophysiological function, using genistein supplementation as an exploratory probe of network-level modulation in the prodromal stage of Alzheimer

1.5 Thesis overview

This doctoral thesis is structured into three experimental studies, each addressing a distinct but complementary aspect of functional network dysfunction in prodromal Alzheimer's disease.

Study 1 is a cross-sectional investigation aimed at characterizing neurophysiological alterations in CSF-confirmed MCI-AD, with particular focus on conventional and high-frequency SEP components as markers of thalamocortical and intracortical network dynamics.

Study 2 is a longitudinal observational study designed to assess the prognostic value of SEP-derived neurophysiological measures, evaluating their ability to predict short-term cognitive decline in patients with MCI-AD.
Study 3 is a randomized controlled trial exploring the effects of chronic genistein supplementation on cognitive outcomes and neurophysiological markers, including high-frequency SEP components and TMS-derived measures of cortical excitability.

Finally, the results of the three studies are integrated and discussed in a General Discussion, which outlines the main implications of the findings, addresses methodological limitations, and proposes future directions for research on functional biomarkers and early intervention strategies in Alzheimer's disease.

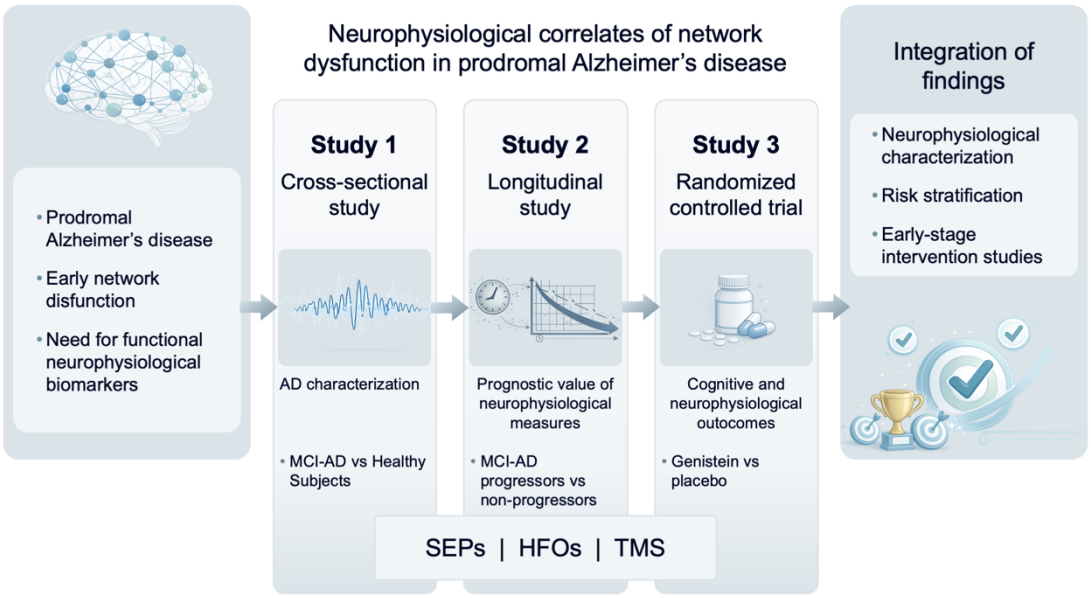

Figure 1. Schematic overview of the thesis rationale and study design.

2. General Methods

2.1 Study design and participants

The present thesis comprises three distinct but theoretically related studies.
The first two studies adopted an observational design. Specifically, **Study 1** is a cross-sectional investigation aimed at comparing neurophysiological and neuropsychological measures between patients with mild cognitive impairment due to Alzheimer's disease (MCI-AD) and healthy control subjects, whereas **Study 2** is a longitudinal observational study designed to investigate neurophysiological changes over time in patients with MCI-AD.
Study 3 is a phase II randomized, double-blind, placebo-controlled clinical trial evaluating the efficacy of genistein supplementation in patients with MCI-AD.
Both longitudinal studies (**Studies 2 and 3**) included a baseline assessment and follow-up visits at 6 and 12 months.
At each time point, comprehensive neurophysiological, clinical, and neuropsychological data were collected.

All patients and healthy control subjects were recruited from the Memory Clinic of the Fondazione Policlinico Universitario Campus Bio-Medico di Roma.
For **Studies 1 and 2**, twenty-one patients diagnosed with (MCI-AD were consecutively recruited between January and June 2022.
The median age of the patient group was 72.0 years (interquartile range [IQR] 9.0).

In **Study 1**, a group of twenty-two healthy adult volunteers was also enrolled to match the median age of the patient group (median age 70.2 years, IQR 7.8).
Exclusion criteria for the healthy control group included pregnancy or breastfeeding, current or recent use of medications known to affect cortical excitability (e.g., antiepileptic drugs, muscle relaxants, benzodiazepines), and any suspected or diagnosed neurological disorder.
To ensure preserved cognitive functioning, only individuals with a Mini-Mental State Examination (MMSE) score of 28 or higher were included.

For **Study 3**, twenty-eight patients with MCI-AD were consecutively recruited between June 2023 and October 2023. The median age of this cohort was 72.0 years (IQR 7.5). Participants were randomly assigned to receive either genistein supplementation (n = 14) or placebo (n = 14).

Across all studies, patients with coexisting neurological disorders or clinical signs of parkinsonism were excluded.

All participants provided written informed consent prior to enrolment.
The study was conducted in accordance with the principles of the Declaration of Helsinki and was approved by the Ethics Committee of the Fondazione Policlinico Universitario Campus Bio-Medico di Roma.

Data were pseudonymized and analysed in compliance with the General Data Protection Regulation (GDPR).

2.2 Diagnosis of MCI due to Alzheimer's disease: Clinical and neurobiological assessment

The diagnosis of mild cognitive impairment due to Alzheimer's disease (MCI-AD) was established according to the 2018 National Institute on Aging–Alzheimer's Association (NIA-AA) Research Framework (Jack et al., 2018).

2.2.1 Neurobiological assessment

For each patient, cerebrospinal fluid (CSF) samples were collected as part of routine clinical practice prior to study enrollment.
CSF concentrations of Aβ42 (Amyloid-β42), Aβ40, t-Tau (total Tau), and p-Tau181 (phosphorylated tau at threonine 181) were measured following standard pre-analytical and analytical protocols (Andreasson et al., 2015).
The CSF samples were collected in sterile polypropylene tubes, immediately centrifuged at 1800 g for 10 minutes at 4°C, aliquoted into polypropylene tubes, and stored at -80°C until analysis.
CSF levels of Aβ42, Aβ40, t-Tau, and p-Tau181 were quantified using commercially available immunoassays (LUMIPULSE, Fujirebio, Japan).

Biological confirmation of Alzheimer's disease pathology was obtained using the AT(N) framework (Jack et al., 2018), which evaluates amyloid pathology (A) through Aβ42 levels and the Aβ42/Aβ40 ratio, tau pathology (T) through p-Tau181, and neurodegeneration (N) through t-Tau concentrations.
Cut-off values provided by the LUMIPULSE platform's manufacturer were used to classify biomarker concentrations as either normal or abnormal (Mj et al., 2019).

2.2.1 Neuropsychological and clinical assessment

All patients and healthy control subjects underwent a comprehensive medical history collection and a standardized neurological examination, aimed at identifying potential exclusion criteria, as well as concomitant medical conditions and ongoing pharmacological treatments.

All subjects included in the three studies underwent a baseline neuropsychological assessment at all study timepoints, consisting of the administration of the Mini-Mental State Examination (MMSE).

In addition, participants enrolled in the randomized controlled trial on genistein supplementation (Study 3) underwent a more extensive neuropsychological evaluation using standardized cognitive and behavioral tests, as detailed below.

2.2.1.1 Mini-Mental State Examination (MMSE)

(Folstein et al., 1975; Tombaugh and McIntyre, 1992)

The MMSE is a global cognitive screening tool designed to assess overall cognitive functioning. It evaluates multiple cognitive domains, including orientation in time and space, immediate and delayed verbal memory, attention and calculation abilities, language functions (comprehension, naming, repetition, reading, and writing), and visuoconstructive skills. The MMSE provides a quantitative measure of global cognitive status and is widely used for the screening and longitudinal monitoring of cognitive impairment.

2.2.1.2 Neuropsychiatric Inventory (NPI)

(Cummings, 1997; Cummings et al., 1994)

The Neuropsychiatric Inventory is a caregiver-based assessment tool designed to evaluate behavioral and psychological symptoms associated with cognitive disorders. It assesses the presence, frequency, and severity of neuropsychiatric symptoms, including to delusions, hallucinations, agitation, depression, anxiety, apathy, irritability, disinhibition, sleep disturbances, and appetite changes. The NPI provides a comprehensive measure of behavioral symptom burden and its impact on patient functioning.

2.2.1.3 Rey Auditory Verbal Learning Test (RAVLT) – 15-Word Test

(Lezak et al., 2012; Rey, 1964; Schmidt, 1996)

The Rey 15-word test evaluates verbal learning and memory processes. Immediate recall trials assess learning efficiency, encoding strategies, and short-term verbal memory. Delayed recall assesses long-term verbal memory retention and consolidation processes. Performance patterns across trials offer insight into learning curves, memory storage, and retrieval abilities.

2.2.1.4 Rey–Osterrieth Complex Figure Test – Figure B (Copy condition)

(Diamond and DeLuca, 1996; Rey, 1941; Shin et al., 2006)

The copy of Figure B of the Rey–Osterrieth Complex Figure Test assesses visuospatial abilities, visuoconstructive skills, and planning strategies. Performance on this task reflects the subject's ability to perceive, organize, and reproduce complex visual information, integrating perceptual accuracy with executive planning components.

2.2.1.5 Digit Span Forward and Backward

(Baddeley, 1992; Sturmey et al., 1993; Wechsler, 1945)

The Digit Span Forward test evaluates attention span and immediate verbal memory by requiring subjects to repeat sequences of digits in the same order as presented.

The Digit Span Backward test assesses working memory and executive control, as it requires the manipulation and reversal of information held in short-term memory. Together, these tasks provide complementary measures of attentional capacity and working memory functioning.

2.3 Neurophysiological Recordings

Both Transcranial Magnetic Stimulation (TMS) and Somatosensory Evoked Potentials (SEPs) were recorded at baseline (T0) for all participants in **Study 1**, and at 6-month and 12-month follow-up visits for patients enrolled in **Studies 2 and 3**.

All neurophysiological measurements were obtained from the dominant hemisphere. This methodological choice was based on previous evidence indicating asymmetric involvement of specific thalamic subnuclei in Alzheimer's disease. In particular, volumetric reductions of the ventral posterolateral (VPL) nucleus, which conveys somatosensory afferent input to the primary somatosensory cortex (S1), have been shown to be more pronounced in the left hemisphere. Such asymmetry supports the hypothesis that functional impairment may preferentially affect the left thalamus during the early stages of the disease (Low et al., 2019).

2.3.1 Somatosensory Evoked Potentials (SEPs)

SEPs were recorded by stimulating the dominant hand's median nerve using an electrical stimulator (DS7A, Digitimer Ltd, UK) through bipolar electrodes at the wrist. The intensity was adjusted to induce a slight painless thumb twitch. Surface Ag/AgCl electrodes were placed at CP3/CP4 and referenced against Fz according to the international 10/20 system. Stimulation was applied at 1.9 Hz, and a total of 1200 stimuli were averaged, bandpass filtered (0.5–2000 Hz), and digitized at 5 kHz using a portable amplifier (BrainVision Recorder, BrainAmp MR plus, Brain products GmBH, Germany, Version:1.10). Recorded SEPs were exported through the BrainVision Analyzer software (Brain products GmBH, Germany, Version:1.05.0005) and visually inspected to reject trials

containing artefacts and to identify key components: N20 peak latency (“N20 latency”, ms), N20 onset-to-peak amplitude (“o-p N20 amplitude”, μV), and N20/P25 peak-to-peak amplitude (“N20/P25 amplitude”, μV).

The data were exported and processed using a semi-automated in-house MATLAB script (The MathWorks Inc., Massachusetts, USA) to extract high-frequency components of the same SEP signal (High-Frequency Oscillations - HFOs). HFOs are rapid bursts of activity, approximately 660 Hz, superimposed on the SEP N20 response following median nerve stimulation (Ozaki and Hashimoto, 2011). These oscillations were isolated from the SEP using a bandpass filter (400-800 Hz) and consist of two components: an early component reflecting thalamocortical pathway activity and a late component generated by cortico-cortical circuits (Ozaki and Hashimoto, 2011).
The area, individual frequency, and duration of the HFOs were calculated from the rectified data within the interval between the onset (i.e., where the signal deflection exceeded 50% of the background noise) and the offset (i.e., where the deflection dropped below 50% of the background noise) of the burst. The HFO area was determined by subtracting the estimated background noise area, which was defined as the area of the rectified wave during a suitable pre-stimulus epoch. If negative values were encountered, the HFO area was set to zero (Capone et al., 2019). The derived variables included the total HFO area ("tot-HFO area", μV/ms), the early component HFO area ("e-HFO area", μV/ms), and the late component HFO area ("l-HFO area", μV/ms) and corresponding durations (ms).

In the present work, the term “conventional SEP components” refers to standard time-domain SEP measures (e.g., N20 latency and amplitude), whereas “high-frequency SEP components (HFOs)” refer to fast oscillatory activity extracted from the same SEP signal.

2.3.2 Transcranial Magnetic Stimulation (TMS)

A TMS-based protocol was conducted at baseline (T0) for all participants, and at follow-up for patients. A figure-of-eight coil with external loop diameters of 9 cm was held over the dominant motor cortex at the optimum scalp position to induce a posterior-anterior current, causing the muscular response of the contralateral first dorsal interosseous (FDI) muscle. Surface muscle responses were obtained via two 9 mm diameter Ag–AgCl electrodes, with the active electrode over the motor point of the muscle and the reference on the metacarpophalangeal joint of the index finger. Muscle responses were amplified and filtered (bandwidth 3–3000 Hz) by D150 amplifiers (Digitimer, Welwyn Garden City, Hertfordshire, UK). During TMS recording, subjects were given audiovisual feedback at high gain to assist in maintaining complete relaxation. Data were collected

on a computer with a sampling rate of 10 kHz per channel and stored for later analysis using a CED 1401 A-D converter (Cambridge Electronic Design, Cambridge, UK).

Several TMS measures were collected:

Resting motor threshold (RMT): the minimal stimulus intensity needed to produce a motor evoked potential (MEP) of ~50 mV in 50% of trials (peak-to-peak amplitude) at rest (Rossini et al., 1994).

Active motor threshold (AMT): the lowest stimulus intensity required to elicit a MEP ≥ 200 μV in 5 out of 10 trials during an isometric contraction of ~10–20% of the maximum voluntary contraction in the target muscle (Rossini et al., 1994).

Motor evoked potentials at 120% RMT (120%RMT-MEPs): Fifteen MEPs were evoked at 120% of RMT intensity, as a global measure of cortical excitability.

Short-latency afferent inhibition (SAI) (Tokimura et al., 2000): SAI is a measure of cholinergic activity performed by pairing electrical stimulation of a peripheral nerve (conditioning stimuli) and cortical stimulation of the motor cortex with TMS (test stimuli). Conditioning stimuli of 200 ms duration were applied through bipolar electrodes to the median nerve at the wrist (cathode proximal). The intensity of the conditioning stimulus was set at just over the motor threshold for evoking a visible twitch of the thenar muscles, while TMS was set to evoke a 1-mV MEP in the target muscle. The interstimulus intervals (ISIs) between conditioning stimulus and TMS were calculated on the individual N20 latency of SEP. Three ISIs were investigated: i) N20 latency +2 ms; ii) N20 latency +3 ms; iii) N20 latency +4 ms (Motolese et al., 2022). Ten stimuli were delivered in a randomized order at each ISI and as test stimulus (without conditioning stimulus). The grand average of conditioned MEP (including all ISIs), measured as peak-to-peak mean amplitude ("SAI mean conditioned MEP", mV) was calculated. The ratio of the SAI-conditioned MEP and the unconditioned MEP ("SAI test MEP", mV) was also calculated ("SAI ratio").

Short latency intracortical inhibition (SICI) and Intracortical Facilitation (ICF): These paired-pulse TMS protocols measure GABAergic and glutamatergic activities, respectively (Di Lazzaro and Ziemann, 2013). For both protocols, two magnetic stimuli are given through the same stimulating coil to investigate the effect of the first (conditioning) stimulus on the second (test) stimulus. In the present study, the conditioning stimulus was set at an intensity of 5% (of stimulator output) below AMT, while TMS was set to evoke a 1-mV MEP in the target muscle. For SICI, a 3 ms ISI was used with a conditioning stimulus set below AMT. For ICF, the ISI was 15 ms. Ten stimuli were delivered in a randomized order at each ISI and as test stimulus (without conditioning stimulus). The ratios between conditioned ("SICI 3ms MEP" and "ICF 15ms MEP", mV) and

unconditioned MEPs ("SICI/ICF test MEP", mV) were calculated for SICI and ICF (respectively "SICI ratio" and "ICF ratio").

2.3.2.1 Repetitive Transcranial Magnetic Stimulation (rTMS) protocol

In participants enrolled in **Study 3**, a repetitive Transcranial Magnetic Stimulation (rTMS) protocol was applied to investigate short-term modulation of motor cortex plasticity.
Specifically, an intermittent theta burst stimulation (iTBS) protocol was delivered over the dominant primary motor cortex (M1).
Stimulation was administered using a Magstim Rapid² Stimulating Unit (Magstim Company Ltd., Whitland, UK) connected to a 70-mm figure-of-eight Air Film Coil (D70mm AFC). The coil was positioned over the optimal scalp location for eliciting MEPs from the contralateral FDI muscle, consistent with the hotspot identified during single-pulse TMS recordings. Coil orientation was maintained to induce a posterior–anterior current flow in the underlying cortex.

The iTBS protocol consisted of bursts of three pulses at 50 Hz, repeated at a frequency of 5 Hz for 10s (for a total of 600 pulses), and was delivered at an intensity corresponding to 80% of the individual AMT. This stimulation intensity was selected in accordance with established safety and efficacy recommendations for theta burst stimulation paradigms (Benavides et al., 2025; Di Lazzaro et al., 2010).

To assess rTMS-induced changes in motor cortex plasticity, MEPs were recorded at an intensity of 120% of the RMT immediately after the completion of the iTBS protocol. Fifteen MEPs were collected and averaged to obtain a reliable post-stimulation measure. The acute effect of iTBS on motor cortical plasticity was quantified by calculating the "ΔMEP", defined as the difference between post-rTMS and baseline 120%RMT-MEP amplitudes. This measure was used as an index of rTMS-induced modulation of corticospinal output.

2.4 Data representation and general statistics

Baseline and follow-up clinical (age, education and MMSE scores), laboratory (CSF Aβ42, CSF Aβ40, CSF Aβ42/40 ratio, CSF tot-Tau, CSF p-Tau) and neurophysiological variables (N20 latency, o-p N20 amplitude, N20/P25 amplitude, tot-HFO area and duration, e-HFO area and duration, l-HFO area and duration, RMT, AMT, 120%RMT-MEPs, SAI-test MEP, SAI-conditioned MEP, SAI ratio, SICI/ICF-test MEP, SICI 3ms MEP, SICI ratio, ICF 15ms MEP, ICF ratio) were expressed as either means ± standard deviation or medians (interquartile range, IQR), depending on

whether they followed a normal distribution, assessed through visual inspection of distribution plots and the Shapiro-Wilk test.

Categorical variables were reported as absolute frequencies and percentages.

A p-value of ≤ 0.05 was considered statistically significant across all analyses.

Statistical analyses were performed using JASP (Version 0.19.1) and Python (Version 3.9.1).

3. Study 1: Cross-sectional comparison between MCI-AD and healthy controls

3.1 Aim and Hypotheses

The aim of **Study 1** was to investigate whether patients with biomarker-confirmed mild cognitive impairment due to Alzheimer's disease (MCI-AD) exhibit neurophysiological alterations when compared to cognitively healthy subjects, focusing on markers of thalamocortical transmission and intracortical excitability.

While structural neuroimaging and fluid biomarkers are well established in identifying Alzheimer's pathology, functional neurophysiological markers remain less explored, particularly during the prodromal stages of the disease. Given the growing conceptualization of Alzheimer's disease as a disorder of large-scale brain networks and synaptic dysfunction, **Study 1** aimed to determine whether subtle functional abnormalities could already be detected at the level of somatosensory processing and cortico-cortical circuits.

The primary hypothesis was that MCI-AD patients would show alterations in high-frequency oscillations (HFOs) extracted from somatosensory evoked potentials, reflecting early dysfunction of thalamocortical pathways. A secondary hypothesis was that measures of cortical excitability and inhibition assessed through transcranial magnetic stimulation would differ between patients and healthy subjects, consistent with early imbalance between excitatory and inhibitory cortical circuits.

3.2 Study Design

Study 1 employed a cross-sectional observational design based on baseline neurophysiological assessments. Comparisons were performed between cognitively healthy subjects and patients with biomarker-confirmed MCI due to Alzheimer's disease.

The focus of the study was not diagnostic classification *per se*, but rather the identification of functional neurophysiological differences that could characterize the prodromal stage of Alzheimer's disease.
All analyses were therefore restricted to baseline data, allowing the evaluation of disease-related alterations independently of longitudinal cognitive decline.

3.3 Statistical Analysis

Given the small sample size and the non-guaranteed normal distribution of neurophysiological variables, between-group comparisons between baseline demographic, clinical, and neurophysiological variables were performed using the Mann–Whitney U test. Categorical variables were analysed using the χ^2-test

The analyses focused on variables derived from somatosensory evoked potentials and HFO extraction, and TMS measures. The analytical strategy was exploratory in nature, aiming to identify neurophysiological parameters that significantly differed between healthy subjects and MCI-AD patients. Statistical significance was defined using a two-tailed threshold of $p \leq 0.05$.

3.4 Results

At baseline, patients with MCI-AD exhibited significant neurophysiological differences compared with healthy subjects (Table 1, Figure 2, and Figure 3).

Variable	HS (n=22)	MCI-AD (n=19)	P-value
Age (y.o.)	70.2 (7.8)	72.1±5.2	0.621
Female sex	13 (59.1%)	8 (42.1%)	0.278
Education (years)	11.7±4.3	12.1±4.4	0.740
MMSE score	30.0 (1.0)	25.0 (4.0)	<.001***
CSF Aβ42 (pg/mL)	N.A.	369.5 (184.3)	-
CSF Aβ40 (pg/mL)	N.A.	6593.0 (2634.3)	-
CSF Aβ42/40 ratio	N.A.	0.060 (0.025)	-
CSF tot-Tau (pg/mL)	N.A.	405.0 (513.0)	-
CSF p-Tau (pg/mL)	N.A.	74.8 (117.8)	-
N20 latency (ms)	19.84±1.36	20.82±1.38	0.072
o-p N20 amplitude (μV)	2.18±1.35	2.87±1.42	0.356
N20/P25 amplitude (μV)	4.59±3.17	5.58±2.67	0.436
HFO freq (Hz)	605.21±69.61	599.73±79.08	0.649
tot-HFO area (AUC, μV/ms)	0.45±0.35	1.28±0.81	0.010*
e-HFO area (AUC, μV/ms)	0.19±0.15	0.33 (0.82)	0.021*
l-HFO area (AUC, μV/ms)	0.28±0.23	0.64 (0.48)	0.032*
tot-HFO duration (ms)	7.92±2.48	14.09±5.18	0.002**
e-HFO duration (ms)	2.02±0.77	5.63±2.81	0.002**
l-HFO duration (ms)	5.66±2.44	8.46±3.76	0.046*
RMT (%)	58.83±11.09	54.39±12.76	0.199
AMT (%)	45.28±8.37	42.78±12.42	0.216
120%RMT MEP (mV)	0.75±0.38	1.02±0.67	0.261
SAI ratio	0.441±0.211	0.580±0.274	0.184
SICI ratio	0.358±0.228	0.563 (0.519)	0.005**
ICF ratio	1.390±0.694	1.264 (0.632)	1.00

Table 1. Baseline demographic, clinical, and neurophysiological characteristics of the study population. *Baseline variables in healthy subjects (HS, n = 22) and patients with mild cognitive impairment due to Alzheimer's disease (MCI-AD, n = 19). Variables are reported as mean ± standard deviation (SD) when normally distributed and as median (interquartile range -IQR) when non-normally distributed; categorical variables are reported as number (percentage). Between-group comparisons were performed using independent-samples statistical tests as appropriate. P-values are reported for comparisons between HS and MCI-AD. Asterisks denote significance levels: p < 0.05 (*), p < 0.01 (**), p < 0.001 (***).* ***Abbreviations:*** *MMSE, Mini-Mental State Examination; CSF, cerebrospinal fluid; pTau, phosphorylated tau at threonine 181; tot-Tau, total tau; Aβ, amyloid-beta; tot-HFO, total high-frequency oscillations; e-HFO, early high-frequency oscillations; l-HFO, late high-frequency oscillations; AUC, area under the curve; RMT, resting motor threshold; AMT, active motor threshold; MEP, motor evoked potential; SAI, short-latency afferent inhibition; SICI, short-interval intracortical inhibition; ICF, intracortical facilitation.*

Conventional SEP parameters, including N20 latency and amplitude, did not differ significantly between groups, indicating preserved integrity of primary somatosensory conduction.
In contrast, high-frequency SEP components (HFOs)-related measures showed clear group differences. MCI-AD patients displayed increased total HFO area with prolonged duration, and analogous changes in both early and late components.
These findings indicate that early-stage Alzheimer's disease is associated with abnormalities in the temporal organization and persistence of high-frequency oscillatory activity, rather than with gross slowing of sensory conduction.

Analysis of TMS parameters revealed selective alterations in sensorimotor integration and intracortical inhibitory circuits. MCI-AD patients showed significant differences in intracortical inhibition measures, including a reduced SICI-related inhibitory effect. In contrast, measures of intracortical facilitation did not show significant differences between groups, nor the SAI related parameters.

Overall, baseline neurophysiological differences between healthy subjects and MCI-AD patients were characterized by prominent alterations in HFO dynamics and selective impairment of inhibitory cortical mechanisms, while basic somatosensory conduction remained preserved.

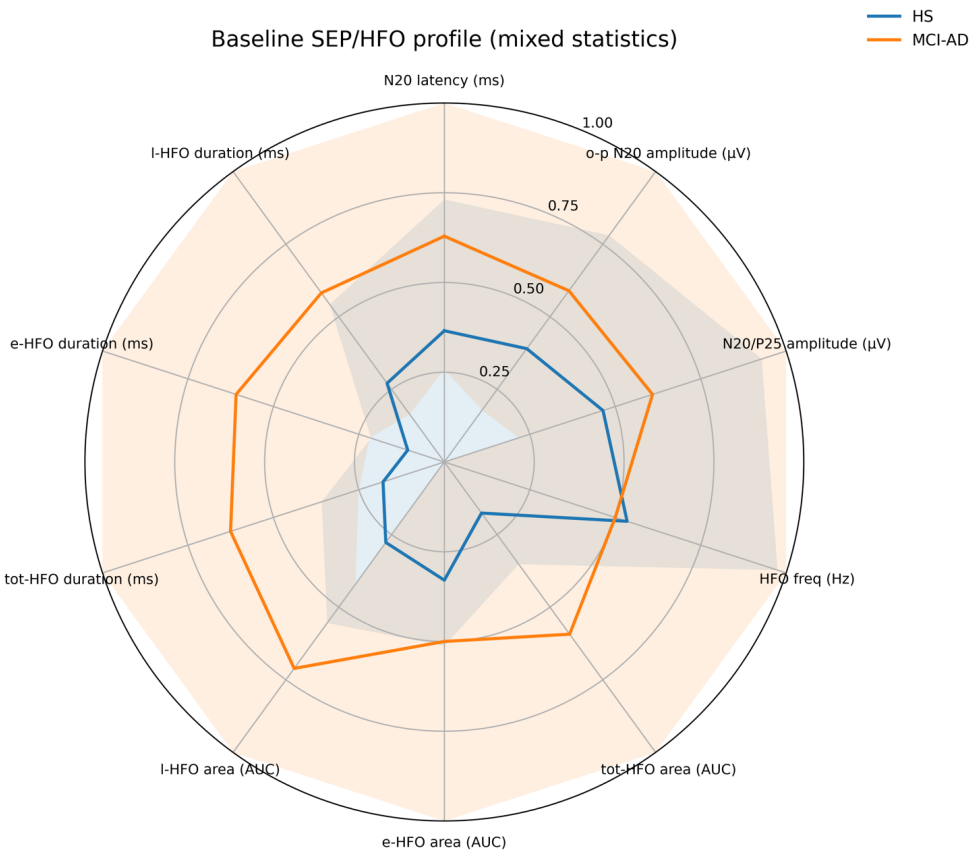

Figure 2. Radar plot using mixed descriptive statistics of SEP/HFO-derived variables (HS vs MCI-AD). *Radar plot illustrating the baseline neurophysiological profiles of healthy subjects (HS) and patients with MCI due to Alzheimer's disease (MCI-AD). For each variable, the solid line represents the central tendency (mean for normally distributed variables; median for non-normally distributed variables), while the shaded area represents dispersion (± standard deviation or interquartile range, respectively). Values were normalized within each variable to allow comparison across measures with different units. Variables included N20 latency, SEP amplitudes, HFO frequency, total/early/late HFO area, and total/early/late HFO duration.* ***Abbreviations:*** *tot-HFO, total high-frequency oscillations; e-HFO, early high-frequency oscillations; l-HFO, late high-frequency oscillations; AUC, area under the curve.*

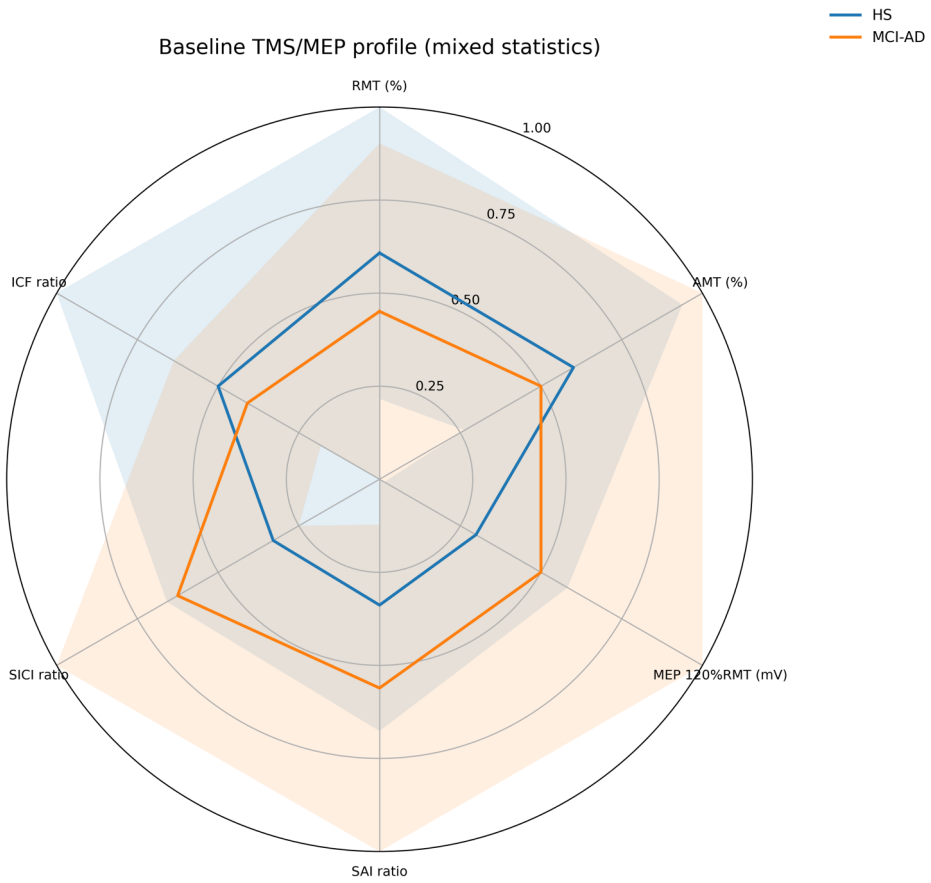

Figure 3. Radar plot using mixed descriptive statistics of TMS-derived variables (HS vs MCI-AD). *Radar plot illustrating baseline TMS–derived measures in healthy subjects (HS) and patients with MCI due to Alzheimer's disease (MCI-AD). For each variable, the solid line represents the central tendency (mean for normally distributed variables; median for non-normally distributed variables), while the shaded area represents dispersion (± standard deviation or interquartile range, respectively). Values were normalized within each variable to enable comparison across measures with different units. Variables included RMT, AMT, MEP amplitude at 120% RMT, SAI ratio, SICI ratio, and ICF ratio.* ***Abbreviations:*** *TMS, transcranial magnetic stimulation; RMT, resting motor threshold; AMT, active motor threshold; MEP, motor evoked potential; SAI, short-latency afferent inhibition; SICI, short-interval intracortical inhibition; ICF, intracortical facilitation.*

3.5 Discussion

The present study demonstrates that patients with biomarker-confirmed mild cognitive impairment due to Alzheimer's disease exhibit distinct baseline neurophysiological alterations compared with cognitively healthy subjects.

A key result of this study is the dissociation between preserved N20 latency and amplitude and marked alterations in high-frequency oscillation (HFO) parameters. While conventional SEP components primarily reflect the integrity and conduction velocity of the lemniscal somatosensory pathway, HFOs are considered sensitive markers of synchronized neuronal firing within thalamocortical and intracortical circuits (Curio et al., 1994; Norata et al., 2024; Ozaki and

Hashimoto, 2011). The observed increase in HFO area and the pronounced prolongation of HFO duration—particularly of the early HFO component—suggest that thalamocortical signalling in MCI-AD is temporally disorganized rather than delayed.

Early HFOs are thought to predominantly reflect presynaptic thalamocortical input and fast excitatory synaptic activity at the cortical level, whereas late HFOs are more closely associated with intracortical processing (Curio et al., 1994; Ozaki and Hashimoto, 2011). The prolongation of both early and late HFO components observed in our cohort of MCI-AD patients may therefore indicate a combined alteration of thalamic drive and cortical network integration. This pattern is consistent with experimental and clinical evidence suggesting early involvement of thalamic nuclei and thalamocortical projections in Alzheimer's disease (Aggleton et al., 2016).

Importantly, the absence of significant differences in HFO frequency suggests that the fundamental oscillatory mechanisms remain preserved, while the temporal persistence and dispersion of oscillatory activity are altered. Such a pattern is compatible with reduced temporal precision and inefficient synchronization of neuronal circuits, a hallmark of early synaptic dysfunction, as previously found in patients with schizophrenia (Uhlhaas and Singer, 2010). From this perspective, prolonged HFO duration may reflect compensatory or maladaptive network responses to early synaptic loss and neurotransmitter imbalance.

In addition to HFO abnormalities, the present study also explored cortical excitability and inhibitory mechanisms using transcranial magnetic stimulation. One of the TMS measures most frequently reported in the literature to distinguish patients with Alzheimer's disease from healthy subjects is short-latency afferent inhibition (SAI), which is typically reduced in Alzheimer's disease as a consequence of early cholinergic dysfunction already evident at prodromal stages (Di Lazzaro et al., 2002, 2000; Guerra et al., 2011; Hampel et al., 2018). In the present cohort, group-level differences in the SAI ratio did not reach statistical significance, likely due to the relatively limited sample size. Nevertheless, the observed trend was consistent with previous findings, with higher SAI ratio values in MCI-AD patients compared with healthy subjects, suggesting less effective sensorimotor inhibition.

Furthermore, alterations in short-interval intracortical inhibition (SICI) were observed, with MCI-AD patients showing reduced inhibitory effects. SICI is primarily mediated by GABA-ergic interneurons (Kujirai et al., 1993), and its reduction has been reported in both Alzheimer's disease and MCI populations (Ferreri et al., 2003). The presence of SICI abnormalities at the prodromal

stage supports the hypothesis that inhibitory circuit dysfunction is an early feature of the disease, potentially contributing to network instability and altered oscillatory dynamics.

The combined SEP/HFO and TMS findings converge toward a model in which early Alzheimer's disease is characterized by impaired inhibitory control and altered thalamocortical synchronization, rather than by isolated deficits in specific pathways. This interpretation is further supported by the radar plot analysis, which highlights a multidimensional neurophysiological profile in MCI-AD patients, with prominent expansion of HFO-related dimensions and selective alterations in inhibitory TMS parameters.

Several limitations of the study should be acknowledged. The relatively small sample size, inherent to neurophysiological investigations, may limit statistical power for detecting subtle effects, particularly for composite measures such as SAI ratios. Moreover, the cross-sectional design precludes direct conclusions regarding the prognostic significance of the observed alterations. These aspects are addressed in the subsequent longitudinal analysis presented in Chapter 4.

In conclusion, **Study 1** provides evidence that sensitive neurophysiological measures reveal early functional alterations in MCI due to Alzheimer's disease that are not detectable using conventional electrophysiological parameters. HFO dynamics and selective inhibitory circuit dysfunction emerge as promising markers of prodromal network impairment, supporting the integration of advanced neurophysiological techniques into the multimodal assessment of early Alzheimer's disease.

4. Study 2: Neurophysiological predictors of short-term clinical progression in MCI due to Alzheimer's disease

4.1 Aim and Hypotheses

The primary aim of **Study 2** was to investigate whether neurophysiological measures are able to predict short-term clinical progression in patients with biomarker-confirmed mild cognitive impairment due to Alzheimer's disease (MCI-AD).

Specifically, this study sought to determine whether alterations assessed through somatosensory evoked potential and measures of cortical excitability, are associated with cognitive decline over a 6-month follow-up period.

Based on the results of **Study 1** and on previous evidence supporting early thalamic and network-level dysfunction in Alzheimer's disease, we hypothesized that a multimodal neurophysiological approach combining SEP and TMS-derived parameters would improve prognostic stratification compared with single-measure analyses.

4.2 Study Design

Study 2 was designed as a longitudinal observational cohort study including patients with biomarker-confirmed MCI due to Alzheimer's disease and cognitively healthy control subjects.

All participants underwent a comprehensive baseline neurophysiological assessment, including somatosensory evoked potentials (SEPs) with high-frequency oscillation analysis and transcranial magnetic stimulation (TMS). Clinical follow-up evaluations were conducted at 6 and 12 months in the MCI-AD group.

Clinical progression was operationally defined as a decline in Mini-Mental State Examination score ("MMSE change") equal to or greater than 0.35 points per month, corresponding to the mean 6-month MMSE variation observed in the cohort. Based on this criterion, MCI-AD patients were classified as progressors or non-progressors.

To maximize sensitivity in a biomarker-defined but numerically limited cohort, neurophysiological observations were aligned with the clinical state closest to progression or non-progression. In cases where follow-up data were available at both 6 and 12 months, patients who progressed only after 12 months were initially analysed as non-progressors at 6 months and subsequently as progressors at

12 months. Each observation was treated as an independent clinical state for group comparisons, reflecting real-world heterogeneity in disease trajectories.

4.3 Statistical Analysis

Group comparisons among healthy subjects, MCI-AD non-progressors, and MCI-AD progressors were performed using non-parametric statistical tests. Specifically, the Kruskal–Wallis test was employed for continuous variables, while categorical variables were analysed using the χ^2-test. When statistically significant differences were identified, Dunn's post-hoc tests with Holm–Bonferroni correction were applied to control for multiple comparisons.

To identify neurophysiological predictors of short-term disease progression, variables showing significant group differences were entered into a feature selection process. Highly correlated variables were identified using Spearman's rank correlation analysis, and within each cluster of interdependent measures, a single representative variable was selected to reduce redundancy.

A logistic regression model was subsequently constructed to evaluate the independent contribution of selected variables to the prediction of 6-month clinical progression. Model performance was assessed using accuracy, sensitivity, specificity, likelihood ratios, and the area under the receiver operating characteristic curve (ROC-AUC).

4.4 Results

4.4.1 Descriptive and inferential statistics

Normality testing, performed using the Shapiro-Wilk test and visual inspection of distribution plots, confirmed that most variables did not follow a normal distribution, justifying the use of non-parametric statistical methods.

Descriptive analysis, expressed as median (IQR), revealed discernible trends across the groups. Kruskal-Wallis tests identified significant group differences in the following neurophysiological parameters: MMSE score ($p < 0.001$), tot-HFO area ($p = 0.007$), early-HFO area ($p = 0.024$), tot-HFO duration ($p < 0.001$), early-HFO duration ($p < 0.001$), late-HFO duration ($p = 0.041$), SICI reduction ($p = 0.047$). Post-hoc Dunn's tests were subsequently performed to identify specific group differences for the statistically significant variables. Results are summarized in Table 2, with Table 3 illustrating post-hoc comparisons.

Variable	HS (n=22)	MCI-AD non-progressors (n=12)	MCI-AD progressors (n=14)	Kruskal-Wallis Statistic	p-value
Age (y.o.)	70.20±7.80	71.33±4.92	73.57±5.36	2.023	0.364
Female sex	13 (59.1%)	3 (25.0%)	7 (50.0%)	1.996 χ^2	0.369
Education (years)	11.70±4.25	13.64±4.43	10.50±4.01	2.448	0.294
MMSE score	30.00 (1.00)	25.00 (4.25)	25.58±2.19	16.703	<.001 ***
CSF Aβ42 (pg/mL)	N.A.	362.16±77.26	438.51±181.21	58.0 MW	0.311
CSF Aβ40 (pg/mL)	N.A.	5800.40±2212.92	7347.12±3500.11	48.0 MW	0.305
CSF Aβ42/40 ratio	N.A.	0.07 (0.03)	0.06±0.02	67.5 MW	0.900
CSF tot-Tau (pg/mL)	N.A.	562.56±292.76	648.15±410.12	60.0 MW	0.577
CSF p-Tau (pg/mL)	N.A.	86.24±58.89	93.00 (120.20)	51.0 MW	0.246
N20 latency (ms)	19.84±1.36	21.00±1.14	20.58±1.54	3.683	0.159
o-p N20 amplitude (μV)	2.18±1.35	2.52±1.12	2.47±1.38	491	0.782
N20/P25 amplitude (μV)	4.59±3.17	5.28±3.38	5.52±2.74	620	0.733
HFO freq (Hz)	605.21±69.61	626.99±82.48	565.18±55.08	3.555	0.169
tot-HFO area (AUC, μV/ms)	0.45±0.35	1.14±0.84	1.69±0.65	10.042	0.007 **
e-HFO area (AUC, μV/ms)	0.19±0.15	0.43±0.31	0.83±0.73	7.448	0.024 *
l-HFO area (AUC, μV/ms)	0.28±0.23	0.71±0.54	0.84±0.70	4.6090	0.100
tot-HFO duration (ms)	7.92±2.48	12.30±7.10	15.82±2.50	14.190	<.001 ***
e-HFO duration (ms)	2.02±0.77	4.32±2.49	6.42±2.45	14.506	<.001 ***
l-HFO duration (ms)	5.66±2.44	7.98±5.38	9.39±3.15	6.384	0.041 *
RMT (%)	58.83±11.09	57.70±10.41	51.92±10.72	3.433	0.180
AMT (%)	45.28±8.37	44.40±8.11	41.00±9.98	1.512	0.469
MEP 120%RMT (mV)	0.75±0.38	0.91 (0.68)	0.88±0.52	3.433	0.180
SAI reduction (%)	44.84±23.21	51.23±17.62	46.52±28.06	229	0.892
SICI reduction (%)	60.27±24.26	56.09 (44.31)	35.69±32.33	6.111	0.047 *
ICF facilitation (%)	30.84±58.45	25.74±42.39	46.21±33.15	2.024	0.364

Table 2. Statistical comparison of demographic, neurophysiological, and biomarker variables across groups.

*The table presents a comparison of various clinical, neurophysiological, and cerebrospinal fluid (CSF) biomarker parameters among Healthy Subjects (HS, n=22), Mild Cognitive Impairment due to Alzheimer's Disease (MCI-AD) non-progressors (n=12), and MCI-AD progressors (n=14). Variables are expressed as mean ± standard deviation when normally distributed, median (interquartile range, IQR) for non-normally distributed variables, and absolute number (%) for categorical variables. Between-group comparisons were performed using the Kruskal-Wallis test, except for categorical variables (e.g., Female sex), which were analysed using the Chi-square test (χ^2), and pairwise comparisons of biomarker values, which were analysed using the Mann-Whitney U test (MW). The Kruskal-Wallis statistic or the respective test statistic is reported along with the p-value. Significant differences are highlighted as follows: $p < 0.05$ (*), $p < 0.01$ (**), and $p < 0.001$ (***). **Abbreviations:** MMSE, Mini-Mental State Examination; CSF, cerebrospinal fluid; pTau, phosphorylated tau at threonine 181; tot-Tau, total tau; Aβ, amyloid-beta; tot-HFO, total high-frequency oscillations; e-HFO, early high-frequency oscillations; l-HFO, late high-frequency oscillations; AUC, area under the curve; RMT, resting motor threshold; AMT, active motor threshold; MEP, motor evoked potential; SAI, short-latency afferent inhibition; SICI, short-interval intracortical inhibition; ICF, intracortical facilitation.*

	Dunn's Post-Hoc Comparisons – p-value		
Variable	**HS vs. MCI-AD non progressors**	**HS vs. MCI-AD progressors**	**MCI-AD non progressors vs. progressors**
MMSE score	<.001 ***	<.001 ***	0.822
tot-HFO area (AUC, μV/ms)	0.051	0.002 **	0.186
e-HFO area (AUC, μV/ms)	0.084	0.008 **	0.377
tot-HFO duration (ms)	0.101	<.001 ***	0.046 *
e-HFO duration (ms)	0.032	<.001 ***	0.112
l-HFO duration (ms)	0.320	0.013 *	0.150
SICI reduction (%)	0.119	0.018 *	0.534

Table 3. Post-hoc Dunn's test results for statistically significant Kruskal-Wallis comparisons.

*This table presents the results of Dunn's post-hoc pairwise comparisons for variables that showed a statistically significant difference in the Kruskal-Wallis test (Table 2). The p-values indicate between-group differences among Healthy Subjects (HS), Mild Cognitive Impairment due to Alzheimer's Disease (MCI-AD) non-progressors, and MCI-AD progressors. P-values have been adjusted for multiple comparisons using the Holm–Bonferroni correction. Significant differences are highlighted as follows: $p < 0.05$ (*), $p < 0.01$ (**), and $p < 0.001$ (***). **Abbreviations:** MMSE, Mini-Mental State Examination; tot-HFO, total high-frequency oscillations; e-HFO, early high-frequency oscillations; l-HFO, late high-frequency oscillations; AUC, area under the curve; SICI, short-interval intracortical inhibition.*

4.4.1 Variable selection for predictive models

To evaluate the predictive capacity of the analysed variables for 6-month disease progression, significant epidemiological and neurophysiological variables were evaluated to be included in a logistic regression.

The MMSE score variable was not included in the predictive model as it was used in the calculation of the outcome variable.

A Spearman's correlation matrix (Table 4) was computed to identify clusters of highly correlated variables (Spearman's $\rho > 0.6$). Within each cluster, the most representative variable was selected for inclusion in the predictive model. For HFO-related variables, we selected total HFO area and early HFO duration, while for TMS-related variables SICI reduction was chosen.

Variable 1	Variable 2	Spearman's ρ	p - value
SICI reduction (%)	tot-HFO area (AUC, µV/ms)	-0.267	0.207
	e-HFO area (AUC, µV/ms)	-0.343	0.119
	tot-HFO duration (ms)	-0.335	0.081
	e-HFO duration (ms)	-0.174	0.376
	l-HFO duration (ms)	-0.340	0.077
tot-HFO area (AUC, µV/ms)	e-HFO area (AUC, µV/ms)	0.809	< .001 ***
	tot-HFO duration (ms)	0.532	0.004 **
	e-HFO duration (ms)	0.568	0.002 **
	l-HFO duration (ms)	0.281	0.155
e-HFO area (AUC, µV/ms)	tot-HFO duration (ms)	0.521	0.006 **
	e-HFO duration (ms)	0.743	< .001 ***
	l-HFO duration (ms)	0.212	0.298
tot-HFO duration (ms)	e-HFO duration (ms)	0.750	< .001 ***
	l-HFO duration (ms)	0.844	< .001 ***
e-HFO duration (ms)	l-HFO duration (ms)	0.357	0.045 *

Table 4. Summary of Spearman's rank correlation coefficients (ρ) and associated p-values between neurophysiological parameters.

*Statistically significant correlations ($p < 0.05$) are highlighted with asterisks: $p < 0.05$ (*), $p < 0.01$ (**), $p < 0.001$ (***). **Abbreviations:** SICI, short-interval intracortical inhibition; tot-HFO, total high-frequency oscillations; e-HFO, early high-frequency oscillations; l-HFO, late high-frequency oscillations; AUC, area under the curve.*

A subsequent feature importance analysis, conducted using the Random Forest model, revealed the relative contribution of each variable to the prediction of disease progression (Figure 4). Among the selected predictors, early-HFO duration emerged as the most influential variable, accounting for 27.32% of the model's predictive power. This was followed by education, which contributed 19.38%, highlighting its substantial role in identifying disease progression. Age also showed a

notable impact, explaining 18.61% of the variability, while SICI reduction and total HFO area accounted respectively for 15.60% and 14.89%, suggesting a moderate but meaningful effect. In contrast, sex demonstrated a minimal contribution (4.21%) and was consequently excluded from the final predictive model to optimize performance.

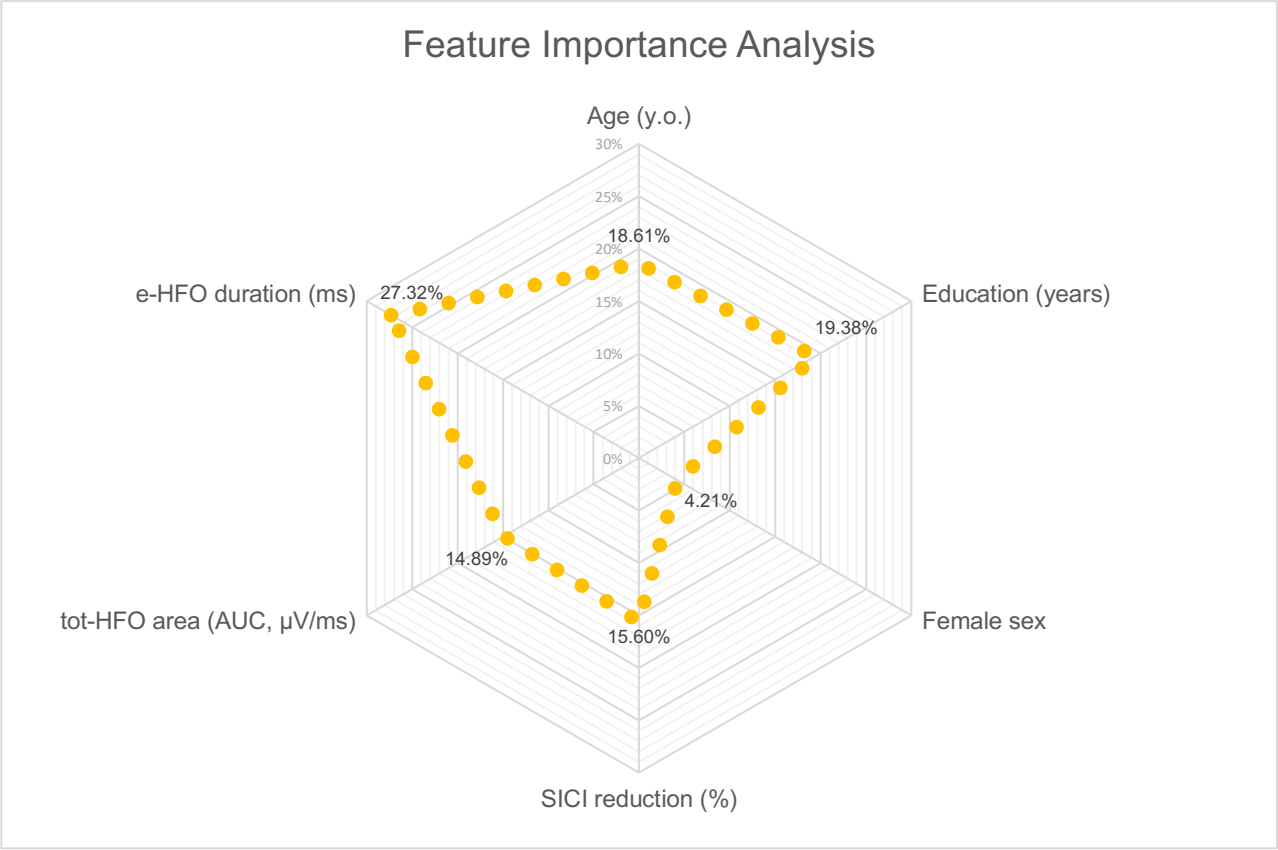

Figure 4. Feature importance in the Random Forest model.
This radar plot displays the relative importance of each predictor in the Random Forest model for forecasting progression at 6 months. Higher values indicate a greater contribution to model predictions. Early HFO duration, SICI reduction, tot-HFO area, Education, and Age showed a notable impact, while Sex demonstrated a minimal contribution. ***Abbreviations:*** *AUC = area under the curve; HFO = high-frequency oscillation; SICI = short-interval intracortical inhibition.*

The final set of selected variables included age, education, SICI reduction, early HFO duration, and total HFO area. Since these variables did not show statistically significant differences between the healthy subjects and the MCI-AD non-progressor group, the two groups were merged into a single category. This approach enabled the identification of disease progression independently of cerebrospinal fluid biomarkers.

The selected variables were incorporated in a logistic regression, to predict progression. Results are summarized in the table below (Table 5):

Independent variables	Odds Ratio	CI Lower	CI Upper	p-value
const	0.036	0.0	17525.332	0.619
Age (y.o.)	1.020	0.861	1.208	0.821
Education (years)	0.889	0.707	1.119	0.318
tot-HFO area (AUC, μV/ms)	1.991	0.524	7.564	0.312
e-HFO duration (ms)	1.733	1.146	2.619	0.009 **
SICI reduction (%)	0.983	0.951	1.016	0.306

Table 5. Logistic regression analysis of predictors for disease progression.
*This table presents the results of a logistic regression model assessing the association between clinical and neurophysiological variables and disease progression at 6 months. The dependent variable is clinical progression in 6 months. Model Fit: Pseudo $R^2 = 0.3564$, suggesting a moderate level of predictive power. Log-Likelihood Ratio Test (LLR p-value) = 0.00094, indicating the model is statistically significant. Results are expressed as Odds Ratios (ORs) with 95% Confidence Intervals (CIs). OR values greater than 1 indicate an increased likelihood of disease progression, while values less than 1 indicate a protective effect. The p-values assess statistical significance, with values <0.05 considered significant. The model suggests that longer e-HFO duration is significantly associated with disease progression ($p = 0.009$), while other variables did not reach statistical significance. Asterisks denote significance levels: $p < 0.05$ (*), $p < 0.01$ (**), $p < 0.001$ (***). **Abbreviations:** SICI, short-interval intracortical inhibition; tot-HFO, total high-frequency oscillations; e-HFO, early high-frequency oscillations; AUC, area under the curve.*

Only early-HFO duration reached statistical significance, indicating that a 1 ms increase in early HFO duration is associated with a 73% increase in the odds of disease progression.

The performance of the model was assessed using multiple metrics, including accuracy, precision, sensitivity, specificity, likelihood ratios, and the area under the receiver operating characteristic curve (ROC-AUC), as summarized in the table below (Figure 5):

Model	Accuracy	ROC-AUC	Precision	Recall (Sensitivity)	Specificity	LR +	LR -
Logistic Regression	0.833	0.870	0.750	64.3%	91.2%	7.286	0.392

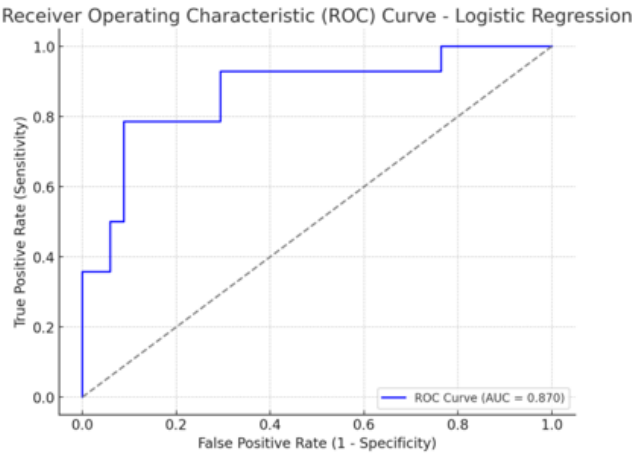

Figure 5. Receiver Operating Characteristic (ROC) curve for logistic regression.
The ROC curve illustrates the diagnostic performance of the model in predicting disease progression at 6 months. The x-axis represents the false positive rate (1 - specificity), while the y-axis represents the true positive rate (sensitivity). The diagonal reference line represents a non-discriminatory model (i.e., a random classifier – Area under the curve, AUC = 0.5). The AUC quantifies the overall discriminative ability of the model, with values closer to 1 indicating better classification performance. With an AUC of 0.875, the logistic regression model demonstrated strong discriminative capability, suggesting a potential utility in predicting disease progression.

Logistic Regression, with an accuracy of 0.833 and a ROC-AUC of 0.870, performed moderately well, with a strong discriminatory power. The model achieved a reasonable balance between sensitivity and specificity, indicating its ability to distinguish between positive and negative cases. It exhibited a high specificity (91.2%), meaning it effectively ruled out false positives. However, its sensitivity (64.3%) suggests that it might miss a significant proportion of actual positive cases. Finally, despite the LR− of 0.392 indicates some risk of false negatives, the LR+ of 7.286 indicates a strong ability to confirm a positive diagnosis, confirming that the model provides at least some diagnostic value in identifying true positives.

4.5 Discussion

Alzheimer's disease is increasingly conceptualized as a disorder characterized by early disruption of large-scale brain networks, rather than as a condition limited to focal regional pathology. Within this framework, the identification of functional biomarkers capable of capturing network-level dysfunction before overt structural damage becomes clinically evident represents a major challenge. In this longitudinal study, we demonstrate that specific neurophysiological measures—most notably the duration of early high-frequency oscillations (e-HFOs)—are able to predict short-term clinical progression in patients with biomarker-confirmed MCI due to Alzheimer's disease.

The most relevant finding of **Study 2** is that baseline prolongation of e-HFO duration significantly predicts cognitive decline over a 6-month follow-up period. Importantly, this effect follows a graded pattern, with a stepwise increase in e-HFO duration from healthy subjects to MCI-AD non-

progressors and, ultimately, to MCI-AD progressors. This continuum strongly suggests that e-HFO prolongation reflects a progressive deterioration of thalamocortical efficiency rather than a late epiphenomenon of advanced neurodegeneration. These findings are in line with neuropathological evidence indicating that thalamic nuclei are involved early in Alzheimer's disease, at stages comparable to hippocampal pathology (Aggleton et al., 2016; Braak and Braak, 1991; Taber et al., 2004).

Early HFOs are widely considered to reflect presynaptic thalamocortical input and fast excitatory synaptic activity at the cortical level (Curio et al., 1994; Ozaki and Hashimoto, 2011). Therefore, the prolongation of e-HFOs observed in MCI-AD progressors is unlikely to be explained by a simple slowing of sensory conduction. Instead, it likely reflects temporal dispersion and sustained activation within thalamocortical circuits, consistent with impaired synchronization and reduced temporal precision of neuronal firing. Experimental studies have shown that thalamic input plays a critical role in regulating cortical states and in shaping the timing of cortical responses, supporting the interpretation of e-HFO alterations as markers of thalamocortical dysregulation (Poulet et al., 2012).

These findings extend and strengthen the observations reported in **Study 1**, in which MCI-AD patients already exhibited marked alterations in HFO area and duration despite preserved conventional SEP components. Together, the two studies support a model in which thalamocortical dysfunction emerges early in the disease course and progressively worsens as patients approach overt cognitive decline. While **Study 1** highlighted the presence of subclinical neurophysiological abnormalities at baseline, Study 2 demonstrates their prognostic relevance, indicating that HFO dynamics are not merely epiphenomenal but carry clinically meaningful information. Similar alterations in SEP-derived HFOs have been reported in other neurological conditions characterized by network-level dysfunction, further supporting their sensitivity as functional markers ((Capone et al., 2019; Insola et al., 2019; Shankar et al., 2021).

From a broader network perspective, the present results are consistent with the growing body of literature describing Alzheimer's disease as a condition characterized by pathological hypersynchrony and altered oscillatory dynamics. Abnormal synchronization and impaired temporal coordination of neuronal activity have been extensively described in neuropsychiatric disorders and are thought to reflect a failure of inhibitory control mechanisms (Uhlhaas and Singer, 2010). In Alzheimer's disease, experimental and clinical evidence suggests that early synaptic dysfunction and neurotransmitter imbalance may lead to compensatory or maladaptive increases in network

synchronization, potentially contributing to disease progression. In this context, the prolongation of early HFO duration observed in MCI-AD progressors may represent an early electrophysiological signature of maladaptive thalamocortical hypersynchrony.

In addition to SEP-derived measures, the present study investigated the contribution of transcranial magnetic stimulation (TMS) parameters to disease progression. Previous studies have consistently reported impairment of short-latency afferent inhibition (SAI) in patients with Alzheimer's disease, interpreting this finding as a neurophysiological marker of central cholinergic dysfunction. However, to date, evidence supporting the use of SAI as a prognostic marker in Alzheimer's disease remains limited. Moreover, the present study cohort reflects a real-life clinical population, in which the majority of patients were receiving acetylcholinesterase inhibitors at the time of neurophysiological assessment. These treatments are known to enhance cholinergic transmission and may partially restore SAI, thereby masking the expected inhibitory deficits. Accordingly, the absence of significant SAI impairment in our findings should be interpreted in light of this relevant pharmacological confound (Di Lazzaro et al., 2004, 2002).
Although alterations in short-interval intracortical inhibition (SICI) were associated with progression risk at the univariate level, they did not retain independent predictive value in the multivariate model. The literature on SICI and intracortical facilitation (ICF) in Alzheimer's disease is heterogeneous, with studies variably reporting reduced inhibition, increased facilitation, or no significant alterations (Freitas et al., 2011). This variability likely reflects differences in disease stage, methodological approaches, and pharmacological status across cohorts. In this context, the lack of robust SICI and ICF alterations in our population may be partly attributable to such heterogeneity, further compounded by the widespread use of cholinergic treatments.

Several methodological strengths of this study should be emphasized. The inclusion of a biomarker-confirmed MCI-AD cohort ensured high diagnostic specificity, while the longitudinal design allowed direct assessment of prognostic relevance. Moreover, the integration of SEP, HFO, and TMS measures provided a comprehensive evaluation of both sensory and motor network function. The feature selection strategy adopted in the statistical analysis reduced redundancy among correlated variables, minimizing the risk of overfitting in a numerically limited sample.

Nevertheless, certain limitations must be acknowledged. The sample size, particularly after stratification into progressors and non-progressors, remains modest and may limit generalizability. Furthermore, the inclusion of multiple observations from some individuals at different follow-up

time points, while increasing sensitivity, introduces potential statistical dependence that cannot be fully controlled. Finally, pharmacological treatment—particularly the widespread use of acetylcholinesterase inhibitors—may have influenced cortical excitability measures, potentially attenuating expected cholinergic effects.

Despite these limitations, the present findings provide compelling evidence that functional neurophysiological markers, and early HFO duration in particular, can capture early network-level dysfunction in Alzheimer's disease and predict short-term clinical progression.
These results support the integration of advanced neurophysiological techniques into multimodal assessment frameworks aimed at early risk stratification, monitoring of disease evolution, and guiding patient selection for disease-modifying interventions.

5. Study 3: Randomized controlled trial on genistein

5.1 Aim and Hypotheses

The primary aim of **Study 3** was to investigate the efficacy and safety of genistein supplementation on cognitive and neuropsychiatric outcomes in patients with mild cognitive impairment due to Alzheimer's disease (MCI-AD) in a real-life, randomized, placebo-controlled setting.

Specifically, this study sought to evaluate whether chronic genistein administration was associated with a slower rate of cognitive decline, as measured by changes in Mini-Mental State Examination (MMSE) scores over time, compared with placebo.
Secondary aims included the assessment of genistein effects on neuropsychiatric symptoms, evaluated through the Neuropsychiatric Inventory (NPI), and the exploration of potential differential effects according to baseline cognitive status.
Given the exploratory nature of the trial, observed effects on secondary outcomes would be considered hypothesis-generating rather than confirmatory.

5.2 Study Design

Study 3 was designed as a randomized, double-blind, placebo-controlled clinical trial conducted in a real-life clinical setting.
Patients with a diagnosis of mild cognitive impairment due to Alzheimer's disease (MCI-AD) were randomly assigned to receive either genistein or placebo and were followed longitudinally with repeated clinical and neuropsychological assessments.

All participants underwent baseline evaluation, including cognitive and neuropsychiatric assessments, before treatment initiation.
Follow-up visits were conducted at predefined time points to assess longitudinal changes in cognitive performance and neuropsychiatric symptomatology.

The trial was conceived as a pilot study, aimed at exploring potential signals of efficacy and feasibility rather than providing definitive evidence of treatment effectiveness. Given the pragmatic nature of the study, patients were allowed to continue standard-of-care treatments, including acetylcholinesterase inhibitors, throughout the study period. This design choice was intended to enhance external validity and to reflect routine clinical practice.

5.3 Statistical Analysis

Descriptive statistics were used to summarize baseline demographic, clinical, and neuropsychological characteristics of the study population.

Baseline comparability between the genistein and placebo groups was assessed using non-parametric statistical tests, given the limited sample size. Specifically, continuous variables were compared using the Mann–Whitney U test, while categorical variables were analysed using χ^2-test.

Given the limited sample size and the exploratory aim of the study, a two-step analytical strategy was adopted to transparently prioritise candidate variables for longitudinal modelling while minimising overfitting.

5.3.1 Estimation-statistics–based screening

As a first step, all available variables—including demographic, clinical, cerebrospinal fluid (CSF), and neurophysiological measures—were screened using estimation statistics (ESCi) in cross-sectional comparisons between treatment groups at the final follow-up visit. For each variable, standardised effect sizes and their corresponding confidence intervals were examined. Variables were ranked according to the magnitude of the effect size and the plausibility of the confidence interval, taking into account both effect size and precision.

This screening procedure was intended solely for prioritisation and not for inferential conclusions. Demographic and clinical variables (e.g., age, education, baseline MMSE), which were expected to show negligible effect sizes due to randomisation, were not considered candidate predictors but were retained as covariates where appropriate.

5.3.2 Longitudinal mixed-effects models

In the second step, selected variables showing the most prominent ESCi patterns were entered individually into linear mixed-effects models (LMMs) to explore their association with cognitive change over time.

The primary outcome was global cognitive performance as measured by the MMSE and was analysed longitudinally using absolute MMSE scores across all visits (T0, T1, and T2). As a robustness analysis, change-from-baseline scores (ΔMMSE) were also modelled, computed as MMSE at each follow-up visit minus baseline MMSE; for ΔMMSE models, only post-baseline observations (T1 and T2) were included, since ΔMMSE is zero by definition at baseline.

Fixed effects included treatment group (genistein vs placebo), time (baseline vs 6 vs 12 months), their interaction, and baseline MMSE, to account for inter-individual differences in initial cognitive status and regression to the mean. Candidate CSF and neurophysiological variables identified in the ESCi screening were entered one at a time as additional fixed effects in exploratory models.

A random intercept for participant was included to account for within-subject correlation across repeated measurements.

The same analytical approach was applied to secondary outcomes, including change in the Neuropsychiatric Inventory total score (NPI and ΔNPI) and other neuropsychological measures. In addition to cognitive and neuropsychiatric outcomes, exploratory longitudinal analyses were conducted to investigate the effects of genistein treatment on neurophysiological markers derived from somatosensory evoked potentials (SEP), high-frequency oscillations (HFOs), cortical excitability, and cortical plasticity. SEP-related measures included N20 latency, N20 onset-to-peak amplitude, and N20–P25 peak-to-peak amplitude. HFO measures comprised frequency, area, and duration of total, early, and late HFO components.

Cortical excitability was assessed using resting motor threshold (RMT), active motor threshold (AMT), motor-evoked potential amplitude at 120% of RMT (MEP), and indices of intracortical inhibition and facilitation, including short-latency afferent inhibition (SAI), short-interval intracortical inhibition (SICI), and intracortical facilitation (ICF). Cortical plasticity was explored through neuromodulation-induced changes in these parameters, expressed as post–pre intervention differences (ΔRMT, ΔAMT, ΔMEP).

For SEP-HFO measures, cortical excitability indices, and plasticity-related outcomes, linear mixed-effects models were fitted using the same general modelling framework described above. Fixed effects included treatment group (genistein vs placebo), time, and their interaction, with adjustment for education, baseline MMSE score, CSF p-tau levels, and selected neurophysiological covariates where appropriate. Subject-specific random intercepts were included to account for within-subject correlations across repeated measurements.

Holm adjustment was applied to post hoc contrasts of estimated marginal means; model-based Type III tests are reported unadjusted. Model parameters were estimated using restricted maximum likelihood, and statistical significance was set at a two-sided α of 0.05.

5.4 Results

5.4.1 Baseline characteristics

A total of 28 participants were included in the analysis, with 14 assigned to the genistein group and 14 to the placebo group. Baseline demographic, clinical, and cerebrospinal fluid characteristics are reported in Table 6, while baseline neurophysiological and neuropsychological variables are reported in Table 7.

Variable	Placebo (N=14)	Genistein (N=14)	p-value
Age (y.o.)	70.357±7.110	71.500±5.880	0.747
Female sex	8 (57.14%)	7 (50.00%)	0.705
Education (years)	12.750±3.980	12.286±4.122	0.815
Disease duration (years)	2.821±1.381	2.0 (1.75)	0.176
CSF Aβ42 (pg/mL)	314.000 (114.000)	340.394±128.875	0.616
CSF Aβ40 (pg/mL)	6928.125±3835.513	5911.893±2235.309	0.631
CSF Aβ42/40 ratio	0.058±0.022	0.063±0.038	0.981
CSF tot-Tau (pg/mL)	590.723±371.658	478.266 200.172	0.625
CSF p-Tau (pg/mL)	100.877±64.542	69.113±40.540	0.202
CSF pTau/Aβ42 ratio	0.289±0.191	0.209±0.089	0.430
Family History of dementia	7 (50.00%)	7 (50.00%)	1.000
Hypertension	8 (57.14%)	9 (64.29%)	0.699
Diabetes Mellitus	1 (7.14%)	2 (14.29%)	0.541
Dyslipidemia	7 (50.00%)	7 (50.00%)	1.000
Coronary Artery Disease (CAD)	1 (7.14%)	0 (0.00%)	0.309
Cerebrovascular Disease	0 (0.00%)	1 (7.14%)	0.309
Antiplatelet Drug	6 (42.86%)	5 (35.71%)	0.699
iAchE	6 (42.86%)	9 (64.29%)	0.256
Memantine	4 (28.57%)	1 (7.14%)	0.139
Antipsychotic	0 (0.00%)	2 (14.29%)	0.142
BZD	1 (7.14%)	1 (7.14%)	1.000
Antidepressant	4 (28.57%)	6 (42.86%)	0.430

Table 6. Statistical comparison of baseline characteristics across groups.
The table presents a comparison of clinical and cerebrospinal fluid (CSF) biomarker parameters in participants assigned to genistein or placebo. Continuous variables are reported as mean ± standard deviation when normally distributed, or as median (interquartile range, IQR) for non-normally distributed variables; categorical variables are reported as n (%). Between-group comparisons were performed using the Mann–Whitney U test for continuous variables and the chi-square test (χ^2) for categorical variables.
Abbreviations: *CSF, cerebrospinal fluid; pTau, phosphorylated tau at threonine 181; tot-Tau, total tau; Aβ, amyloid-beta; iAchE, acetylcholinesterase inhibitors; BZD, benzodiazepines.*

Variable	Placebo (N=14)	Genistein (N=14)	p-value
MMSE baseline	24.714±2.998	25.429±2.954	0.514
AVLT sum 1-5 baseline	29.300±13.005	24.846±10.057	0.685
AVLT delay baseline	4.556±4.503	2.00 (3.00)	0.199
Digit span forward baseline	5.000 (0.000)	4.500 (3.000)	0.459
Digit span backward baseline	3.000 (1.000)	2.750±1.422	0.263
ROCF copy baseline	28.950±7.009	29.604±5.414	0.895
NPI baseline	10.00 (13.50)	6.00 (14.00)	0.793
N20 latency (ms)	20.523±1.425	20.683±1.309	0.624
o-p N20 amplitude (μV)	2.719±1.737	2.354±0.976	0.979
N20/P25 amplitude (μV)	5.071±2.707	4.673±1.672	0.935
HFO freq (Hz)	587.914±74.423	572.826±108.234	1.000
tot-HFO area (AUC, μV/ms)	0.877±0.696	0.996±0.723	0.728
e-HFO area (AUC, μV/ms)	0.203 (0.470)	0.298±0.188	0.810
l-HFO area (AUC, μV/ms)	0.532±0.352	0.394 (0.760)	0.683
tot-HFO duration (ms)	10.677±4.343	9.400 (2.400)	0.978
e-HFO duration (ms)	2.400 (2.600)	2.800 (1.500)	0.662
l-HFO duration (ms)	7.215±3.481	6.800 (2.723)	0.870
RMT	54.429±12.617	60.333±15.293	0.236
AMT	41.857±11.844	49.250±12.990	0.099
MEP 120%RMT	0.933±0.494	1.107±0.740	0.728
SAI ratio	0.591±0.285	0.375±0.157	0.056
SICI ratio	0.750 (0.470)	0.668±0.390	0.852
ICF ratio	1.536±0.652	1.456±0.461	0.954
ΔRMT	55.326±12.742	60.304±16.128	0.750
ΔAMT	42.005±10.355	48.050±13.137	0.449
ΔMEP	0.029±0.487	0.028±0.530	0.332

Table 7. Statistical comparison of baseline neuropsychological and neurophysiological measures across groups.

The table presents a comparison of baseline cognitive, neuropsychiatric, and neurophysiological measures between participants assigned to genistein or placebo treatment. Continuous variables are reported as mean ± standard deviation when normally distributed, or as median (interquartile range, IQR) for non-normally distributed variables, while p values refer to between-group comparisons. Given the small sample size, between-group differences were assessed using the Mann–Whitney U test for all continuous variables.

Abbreviations: *MMSE, Mini-Mental State Examination; AVLT, Auditory Verbal Learning Test; ROCF, Rey–Osterrieth Complex Figure; NPI, Neuropsychiatric Inventory; SEP, somatosensory evoked potentials; HFO, high-frequency oscillations; e-HFO, early high-frequency oscillations; l-HFO, late high-frequency oscillations; AUC, area under the curve; RMT, resting motor threshold; AMT, active motor threshold; MEP, motor evoked potential; SAI, short-latency afferent inhibition; SICI, short-interval intracortical inhibition; ICF, intracortical facilitation.*

Baseline characteristics were comparable between the genistein and placebo groups (Table 6).

Median age did not differ significantly between groups (70.4 ± 7.1 years vs 71.5·± 5.9 years;

p=0.747), nor did the proportion of women (50.0% vs 57.1%; p=0.705). Educational attainment (p=0.815), and disease duration (p=0.176) were also similar between groups. No statistically significant between-group differences were observed in cerebrospinal fluid biomarkers, including Aβ42 (p=0.616), Aβ40 (p=0.631), the Aβ42/40 ratio (p=0.981), total tau (p=0·625), phosphorylated tau (p=0.202), or the p-tau/Aβ42 ratio (p=0.430). The prevalence of vascular risk factors, family history of dementia, and concomitant medications, including cholinesterase inhibitors and memantine, did not differ significantly between treatment arms (all p>0.05), indicating a good baseline balance between groups.

Baseline neuropsychological and neurophysiological measures were also comparable between the genistein and placebo groups (Table 7). No statistically significant between-group differences were observed in baseline cognitive performance across global cognition, memory, executive function, visuospatial abilities, or neuropsychiatric symptoms (all p>0.05). Similarly, baseline somatosensory evoked potentials, high-frequency oscillatory components, and measures of cortical excitability and plasticity did not differ significantly between treatment arms (all p>0.05). Of note, a borderline between-group difference was observed for the short-latency afferent inhibition (SAI) ratio, which was numerically higher in the placebo group compared with the genistein group (0.591 ± 0.285 vs 0.375 ± 0.157; Mann–Whitney U test, p = 0.056). Overall, these findings indicate a balanced distribution of baseline neuropsychological and neurophysiological measures between groups.

Estimation-statistics screening revealed substantial heterogeneity across candidate variables. As expected, demographic, clinical, neuropsychological, and baseline neurophysiological measures showed negligible standardised effect sizes, with confidence intervals largely centred around zero, consistent with appropriate randomisation and absence of meaningful baseline imbalance.

5.4.2 Estimation statistics at T2

Based on cross-sectional estimation-statistics analyses comparing genistein and placebo at the 12-month follow-up (T2), several CSF and neurophysiological variables exhibited standardized effect sizes of moderate magnitude, albeit with wide confidence intervals indicating limited precision (Table 8). These patterns were not interpreted inferentially but were used to prioritise candidate covariates for subsequent exploratory longitudinal models. Education, CSF phosphorylated tau, late HFO duration, baseline MMSE, and neuromodulation-induced change in MEP amplitude (ΔMEP) were therefore selected for modelling.

Baseline MMSE was included as a covariate in models where the dependent outcome was not neuropsychological. ΔMEP was entered as a covariate only when it did not constitute the dependent outcome and when the outcome variable was not directly derived from TMS measures. Finally, late

HFO duration was not added as an extra covariate in SEP–HFO models to avoid circularity/overadjustment, but it was retained as a covariate in models targeting neuropsychological and other neurophysiological outcomes.

Rank	Variable	SMD d_s	95% CI
1	Education (years)	−0.738	−1.64 ; 0.18
2	CSF p-Tau (pg/mL)	−0.704	−1.58 ; 0.19
3	CSF pTau/Aβ42 ratio	−0.600	−1.47 ; 0.28
4	l-HFO duration (ms)	+0.595	−0.39 ; 1.56
5	MMSE baseline	+0.566	−0.32 ; 1.43
6	ΔMEP	−0.558	−1.56 ; 0.46
7	Age (years)	+0.517	−0.34 ; 1.36
8	CSF Aβ40 (pg/mL)	−0.514	−1.40 ; 0.39
9	CSF tot-Tau (pg/mL)	−0.499	−1.39 ; 0.40
10	e-HFO area (AUC)	−0.500	−1.46 ; 0.48
11	tot-HFO duration (ms)	+0.474	−0.50 ; 1.43
12	tot-HFO area (AUC)	−0.408	−1.37 ; 0.56
13	SICI ratio	−0.386	−1.40 ; 0.65
14	HFO frequency (Hz)	−0.371	−1.33 ; 0.60
15	CSF Aβ42 (pg/mL)	−0.372	−1.23 ; 0.50
16	l-HFO area (AUC)	−0.336	−1.29 ; 0.63
17	CSF Aβ42/40 ratio	+0.278	−0.59 ; 1.14
18	SAI ratio	−0.235	−1.19 ; 0.73
19	Female sex	−0.170	−1.01 ; 0.67
20	ICF ratio	+0.192	−0.83 ; 1.21
21	ΔRMT	−0.113	−1.15 ; 0.92
22	ΔAMT	−0.063	−1.10 ; 0.97
23	e-HFO duration (ms)	−0.083	−1.03 ; 0.87

Table 8. Estimation statistics at T2 (Genistein vs Placebo)

Standardized mean differences (SMD d_s) with 95% confidence intervals are reported for between-group comparisons at the 12-month follow-up (T2). Effect sizes quantify the magnitude and direction of group differences (positive values indicate higher values in the genistein group). Confidence intervals reflect estimation uncertainty and are not intended for hypothesis testing. Variables are ordered by the absolute magnitude of the standardized effect size. Notes: (i) This standardized mean difference is called d s because the standardizer used was s_p; (ii) d_s has been corrected for bias. Underlined variables denote those entered into the linear mixed-effects models. ***Abbreviations:*** *MMSE, Mini-Mental State Examination; CSF, cerebrospinal fluid; pTau, phosphorylated tau at threonine 181; tot-Tau, total tau; Aβ, amyloid-beta; tot-HFO, total high-frequency oscillations; e-HFO, early high-frequency oscillations; l-HFO, late high-frequency oscillations; AUC, area under the curve; RMT, resting motor threshold; AMT, active motor threshold; MEP, motor evoked potential; SAI, short-latency afferent inhibition; SICI, short-interval intracortical inhibition; ICF, intracortical facilitation.*

5.4.3 Primary outcome: MMSE

Linear mixed-effects models were used to examine longitudinal changes in cognitive performance as measured by the Mini-Mental State Examination (MMSE). Models included fixed effects for treatment group, time, and their interaction, with subject-specific random intercepts. Analyses were performed using both absolute MMSE values and change scores (ΔMMSE) to assess robustness to alternative model specifications (Table 9).

	Fixed effect	Estimate	SE	df	t	p-value
A. Absolute MMSE	*Intercept*	22.110	3.744	24.47	5.905	< 0.001
	Education (years)	0.107	0.257	19.03	0.417	0.681
	CSF pTau (pg/mL)	0.002	0.018	16.59	0.088	0.931
	l-HFO duration (ms)	0.226	0.222	27.03	1.022	0.316
	ΔMEP	0.514	0.836	26.40	0.614	0.544
	Timing (T1 vs T0)	1.414	1.747	17.64	0.810	0.429
	Timing (T2 vs T0)	-0.246	1.917	18.38	-0.128	0.899
	Treatment	-0.820	1.974	21.92	-0.415	0.682
	Timing (T1) ✻ Treatment	-4.803	2.293	17.85	-2.094	0.051
	Timing (T2) ✻ Treatment	-2.758	2.523	21.05	-1.093	0.287
B. ΔMMSE	*Intercept*	-27.901	16.862	7.346	-1.655	.140
	Education (years)	0.160	0.382	7.488	0.419	.687
	l-HFO duration (ms)	-0.327	0.320	6.162	-1.021	.346
	ΔMEP	1.155	0.953	9.725	1.211	.254
	CSF pTau (pg/mL)	0.003	0.021	7.436	0.166	.873
	MMSE baseline	1.131	0.630	7.285	1.795	.114
	Timing (T2 vs T1)	-1.096	1.601	4.595	-0.685	.526
	Treatment	-7.289	2.522	9.400	-2.890	.017*
	Timing ✻ Treatment	1.977	2.189	4.813	0.903	.409

Table 9. Linear mixed-effects models for MMSE outcomes.

Results of linear mixed-effects models examining longitudinal changes in cognitive performance as measured by the Mini-Mental State Examination (MMSE). Panel A reports results for absolute MMSE scores, while Panel B reports results for change in MMSE from baseline (ΔMMSE). All models included subject-specific random intercepts and fixed effects for treatment group, time, and their interaction, together with selected covariates. Factor levels were parameterised using treatment contrast coding; therefore, main effects are conditional on the reference level of the interacting factor. Degrees of freedom were estimated using the Satterthwaite approximation. P-values are reported for descriptive purposes and should be interpreted in conjunction with effect sizes and confidence intervals. ***Abbreviations:*** *CSF, cerebrospinal fluid; pTau, phosphorylated tau; HFO, high-frequency oscillations; l-HFO, late component of high-frequency oscillations; MEP, motor evoked potential.*

In analyses of absolute MMSE scores (Table 9, Panel A; Figure 6), no statistically robust main effect of treatment was observed. However, a borderline treatment-by-time interaction emerged at one follow-up time point ($p = 0.051$), with the direction of the effect indicating a less pronounced decline in the genistein group compared with placebo. Although this interaction did not reach conventional levels of statistical significance and was associated with wide standard errors, the magnitude and direction of the estimate suggest a potential treatment-related signal, warranting cautious interpretation. None of the included covariates, including years of education, CSF p-tau levels, late HFO duration, or neuromodulation-induced changes in motor evoked potential amplitude, showed a statistically supported independent association with absolute MMSE scores.

When modelling change in MMSE from baseline (ΔMMSE) (Table 9, Panel B), a significant main effect of treatment was observed, indicating a difference in average cognitive change between groups across the follow-up period. Importantly, the absence of a significant treatment-by-time interaction suggests that this effect reflects a global difference in cognitive change rather than a divergence in longitudinal trajectories. Baseline MMSE and other covariates did not show statistically supported independent associations with ΔMMSE.

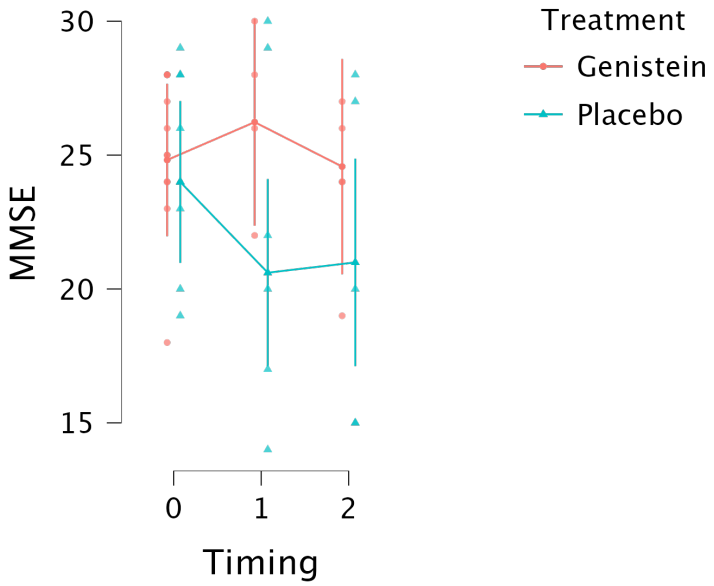

Figure 6. Longitudinal mixed-effects model–based trajectories of MMSE by treatment group. *Observed individual Mini-Mental State Examination (MMSE) scores (symbols) and model-based estimated marginal means with 95% confidence intervals (lines and error bars) derived from linear mixed-effects modelling are shown for the genistein and placebo groups across study visits (T0, baseline; T1, 6 months; T2, 12 months). Models included fixed effects for treatment, time, and their interaction, together with selected covariates, and subject-specific random intercepts. While both groups exhibited changes in MMSE over time, trajectories appeared directionally different, with a less pronounced decline in the genistein group at later follow-up. Substantial inter-individual variability and overlapping confidence intervals indicate limited estimation precision; therefore, the figure is intended to illustrate longitudinal data patterns rather than provide inferential evidence.*

Overall, while the present analyses do not provide definitive evidence of a differential longitudinal effect of genistein on MMSE trajectories, the convergent directionality of treatment-related estimates across model specifications, together with a borderline interaction in the absolute MMSE model, suggests the presence of a weak but coherent signal that may be obscured by limited sample size and estimation precision. These findings support further investigation in adequately powered studies.

5.4.4 Secondary main outcome: Neuropsychiatric Inventory (NPI)

Linear mixed-effects models were used to evaluate longitudinal changes in neuropsychiatric symptom burden as assessed by the Neuropsychiatric Inventory (NPI). Models included fixed effects for treatment group, time, and their interaction, together with selected demographic, biological, and neurophysiological covariates, and subject-specific random intercepts.

In analyses of absolute NPI scores (Table 10, Panel A; Figure 7), no statistically significant main effect of treatment or treatment-by-time interaction was observed. Both timing contrasts indicated a numerical increase in NPI scores over follow-up, consistent with a worsening of neuropsychiatric symptoms over time; however, these effects did not reach statistical significance. Among covariates, years of education showed a borderline negative association with NPI scores ($p = 0.055$), suggesting lower symptom burden in individuals with higher educational attainment, although this effect was imprecisely estimated. No significant associations were observed for CSF tau levels or neurophysiological measures.
Importantly, no longitudinal divergence between treatment groups was observed, indicating that changes in neuropsychiatric symptoms over time did not differ between genistein and placebo.

Consistent findings were obtained when modelling change in NPI from baseline (ΔNPI) (Table 10, Panel B). Neither the main effect of treatment nor the treatment-by-time interaction reached statistical significance, indicating the absence of differential longitudinal changes in neuropsychiatric symptoms between the genistein and placebo groups. Baseline NPI and other covariates were not significantly associated with ΔNPI, and estimates were characterised by wide standard errors, reflecting limited precision.

Overall, longitudinal mixed-effects analyses of NPI outcomes did not provide evidence of a treatment-related modulation of neuropsychiatric symptoms. The observed increase in symptom burden over time appeared to occur similarly in both treatment groups, in line with the pattern illustrated in Figure 7.

	Fixed effect	Estimate	SE	df	t	p-value
A. Absolute NPI	*Intercept*	32.757	10.883	26.00	3.010	.006
	Education (years)	-1.337	0.666	26.00	-2.007	.055
	CSF pTau (pg/mL)	0.009	0.044	26.00	0.200	.843
	l-HFO duration (ms)	-0.400	0.780	26.00	-0.513	.612
	ΔMEP	-0.333	4.045	26.00	-0.082	.935
	Timing (T1 vs T0)	-9.732	6.976	26.00	-1.395	.175
	Timing (T2 vs T0)	-7.460	8.148	26.00	-0.916	.368
	Treatment	-6.351	5.717	26.00	-1.111	.277
	Timing (T1) ✻ Treatment	15.607	9.884	26.00	1.579	.126
	Timing (T2) ✻ Treatment	14.174	11.896	26.00	1.191	.244
B. ΔNPI	*Intercept*	40.989	36.270	5.000	1.130	.310
	Education (years)	-2.399	2.181	5.000	-1.100	.322
	l-HFO duration (ms)	-1.602	2.461	5.000	-0.651	.544
	ΔMEP	0.054	0.129	5.000	0.419	.693
	CSF pTau (pg/mL)	-1.919	1.503	5.000	-1.277	.258
	NPI baseline	-8.415	9.233	5.000	-0.911	.404
	Timing (T2 vs T1)	-1.363	11.804	5.000	-0.115	.913
	Treatment	5.257	11.208	5.000	0.469	.659
	Timing ✻ Treatment	5.513	21.447	5.000	0.257	.807

Table 10. Linear mixed-effects models for Neuropsychiatric Inventory (NPI) outcomes.

Results of linear mixed-effects models examining longitudinal changes in neuropsychiatric symptom burden as measured by the Neuropsychiatric Inventory (NPI). Panel A reports results for absolute NPI total scores, while Panel B reports results for change in NPI from baseline (ΔNPI). All models included subject-specific random intercepts and fixed effects for treatment group, time, and their interaction, together with selected demographic, biological, and neurophysiological covariates. Degrees of freedom were estimated using the Satterthwaite approximation. P-values are reported for descriptive purposes and should be interpreted in conjunction with effect sizes and confidence intervals. ***Abbreviations:*** *CSF, cerebrospinal fluid; pTau, phosphorylated tau; HFO, high-frequency oscillations; MEP, motor evoked potential.*

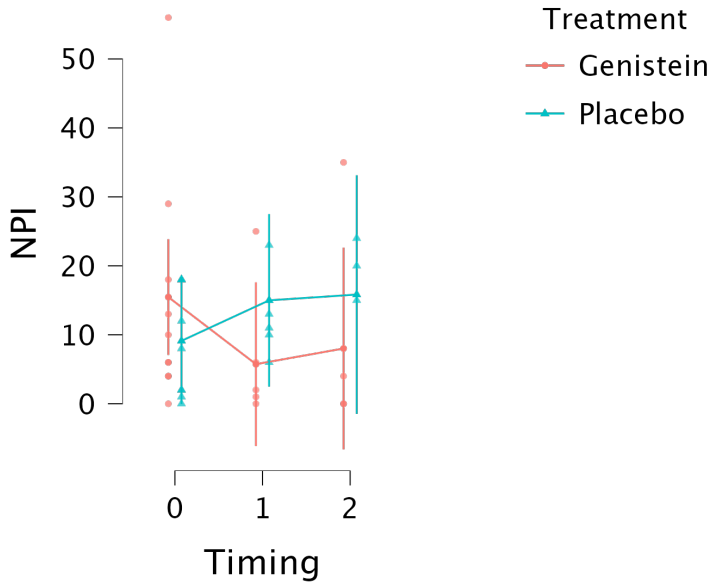

Figure 7. Longitudinal mixed-effects model–based trajectories of NPI by treatment group
Individual Neuropsychiatric Inventor (NPI) scores (symbols) and model-based estimated marginal means with 95% confidence intervals (lines and error bars) derived from linear mixed-effects modelling are shown for the genistein and placebo groups across study visits (T0, baseline; T1, 6 months; T2, 12 months). Models included fixed effects for treatment, time, and their interaction, together with selected covariates, and subject-specific random intercepts. Although neuropsychiatric symptom burden increased over time in both groups, no clear divergence in longitudinal trajectories between treatment groups was observed. Considerable inter-individual variability and overlapping confidence intervals indicate substantial estimation uncertainty; therefore, the figure is intended to illustrate longitudinal data patterns rather than provide inferential evidence.

5.4.5 Other neuropsychological outcomes

Linear mixed-effects models were used to examine longitudinal changes in secondary neuropsychological outcomes, including verbal memory, attention, working memory, and visuoconstructive abilities, using absolute test scores.
Models included fixed effects for treatment group, time, and their interaction, together with selected demographic, biological, and neurophysiological covariates, and subject-specific random intercepts.

For verbal learning performance (AVLT 1-5 sum), no significant main effects of treatment or time were observed, nor was there evidence of a treatment-by-time interaction. Estimated marginal means suggested broadly stable performance over follow-up in both groups, with overlapping confidence intervals across time points. Similarly, Digit Span forward, indexing attention and short-term memory, did not show significant longitudinal changes or treatment-related effects.

In contrast, AVLT delayed recall and Digit Span backward, reflecting delayed verbal memory and working memory, respectively, showed a significant main effect of time, indicating changes in performance over follow-up independent of treatment group. However, no significant main effect of

treatment or treatment-by-time interaction was detected for these outcomes, suggesting that observed temporal changes occurred similarly in the genistein and placebo groups.

Finally, visuoconstructive performance assessed by the Rey–Osterrieth Complex Figure copy did not exhibit significant effects of treatment, time, or their interaction. A borderline association between CSF tau levels and ROCF copy performance was observed, although this effect was imprecisely estimated and did not reach conventional levels of statistical significance.

Overall, analyses of secondary neuropsychological outcomes did not provide evidence of treatment-related modulation of cognitive performance beyond global cognition, with longitudinal patterns largely driven by time-dependent changes and substantial inter-individual variability, as illustrated in Figure 8.

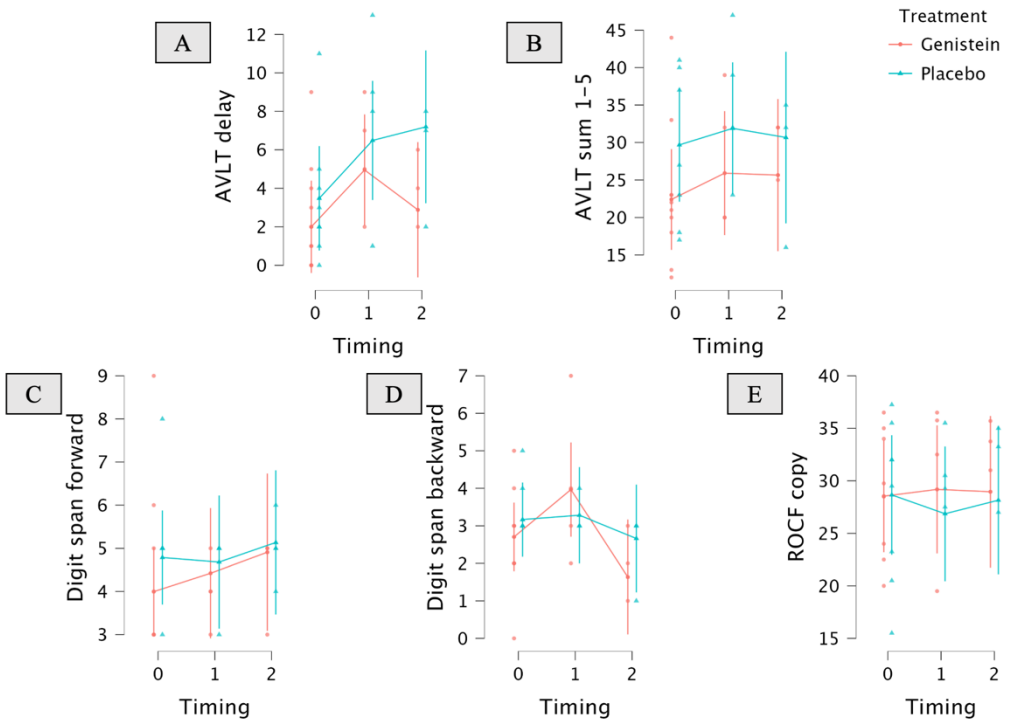

Figure 8. Longitudinal mixed-effects model–based trajectories of secondary neuropsychological outcomes.

Observed individual scores (symbols) and model-based estimated marginal means with 95% confidence intervals (lines and error bars) derived from linear mixed-effects models are shown for secondary neuropsychological outcomes in the genistein and placebo groups across study visits (T0, baseline; T1, 6 months; T2, 12 months). Panels display (A) AVLT delayed recall, (B) AVLT total learning (trials 1–5), (C) Digit Span forward, (D) Digit Span backward, and (E) Rey–Osterrieth Complex Figure (ROCF) copy. All models included fixed effects for treatment group, time, and their interaction, together with selected demographic, biological, and neurophysiological covariates, and subject-specific random intercepts. Across outcomes, substantial inter-individual variability and largely overlapping confidence intervals were observed, indicating limited estimation precision and the absence of robust treatment-related effects. The figure is intended to illustrate longitudinal data patterns rather than provide inferential evidence.

5.4.6 Effects of treatment on SEP and SEP-related high-frequency oscillations

Linear mixed-effects models were used to examine whether genistein modulated conventional SEP measures and high-frequency SEP components (HFOs) over time, adjusting for education, baseline MMSE, CSF phosphorylated tau, and neuromodulation-induced change in MEP amplitude (ΔMEP), with subject-specific random intercepts.

Across conventional SEP measures, N20 latency and onset-to-peak N20 amplitude showed no significant main effects of treatment or timing and no evidence of a timing-by-treatment interaction (all $p>0.05$). Similarly, HFO frequency did not exhibit treatment- or time-dependent modulation; however, baseline MMSE was positively associated with HFO frequency ($F=6.232$, $p=0.029$), indicating higher frequency values in participants with higher baseline global cognitive status, independent of treatment allocation.

Peak-to-peak N20–P25 amplitude demonstrated a significant main effect of timing, with both post-baseline contrasts indicating a reduction relative to baseline (Timing 1: estimate −1.818, $p=0.022$; Timing 2: estimate −1.947, $p=0.020$), without evidence of treatment-related divergence (timing-by-treatment $p=0.278$).

For high-frequency SEP components, total HFO area showed a significant main effect of timing, reflecting a reduction over follow-up (Timing 1: estimate -0.893, $p=0.007$; Timing 2: estimate -0.960, $p=0.017$), together with a timing-by-treatment interaction that approached statistical significance. Notably, a significant interaction was observed at the first follow-up (T1×Treatment: estimate 0.875, $p=0.038$), indicating an early divergence between genistein and placebo after adjustment for education, baseline MMSE, CSF p-tau levels, and ΔMEP. This effect was not maintained at the final follow-up (T2×Treatment: estimate 0.210, $p=0.684$), suggesting a transient or non-linear modulation rather than a sustained treatment-related change.

In parallel, late HFO duration exhibited a borderline timing-by-treatment interaction at the second follow-up (T2×Treatment: estimate −3.396, $p=0.059$), with directionally consistent estimates. Although neither measure demonstrated a robust or persistent treatment effect, the temporal convergence of an early signal in total HFO area and a later trend in l-HFO duration supports the presence of a subtle, time-dependent modulation of SEP–HFO dynamics associated with genistein treatment.

Early HFO area showed a significant treatment effect in the Type III test ($F=5.345$, $p=0.029$); however, the fixed-effect coefficient for treatment was not statistically supported in the parameter estimates (estimate 0.133, $p=0.344$) and the timing-by-treatment interaction was not significant

(p=0.453). This discordance, together with the warning of a singular model fit, suggests limited stability of the estimated effects.

No statistically supported treatment-related effects were observed for late HFO area, while duration-based indices showed no robust treatment effects, while total HFO duration changed over time (F=5.092, p=0.015).

Overall, the SEP–HFO findings do not demonstrate a robust treatment effect, but they suggest a potential early signal on total HFO area with directionally convergent (borderline) changes in the duration of the late component (Figure 9).

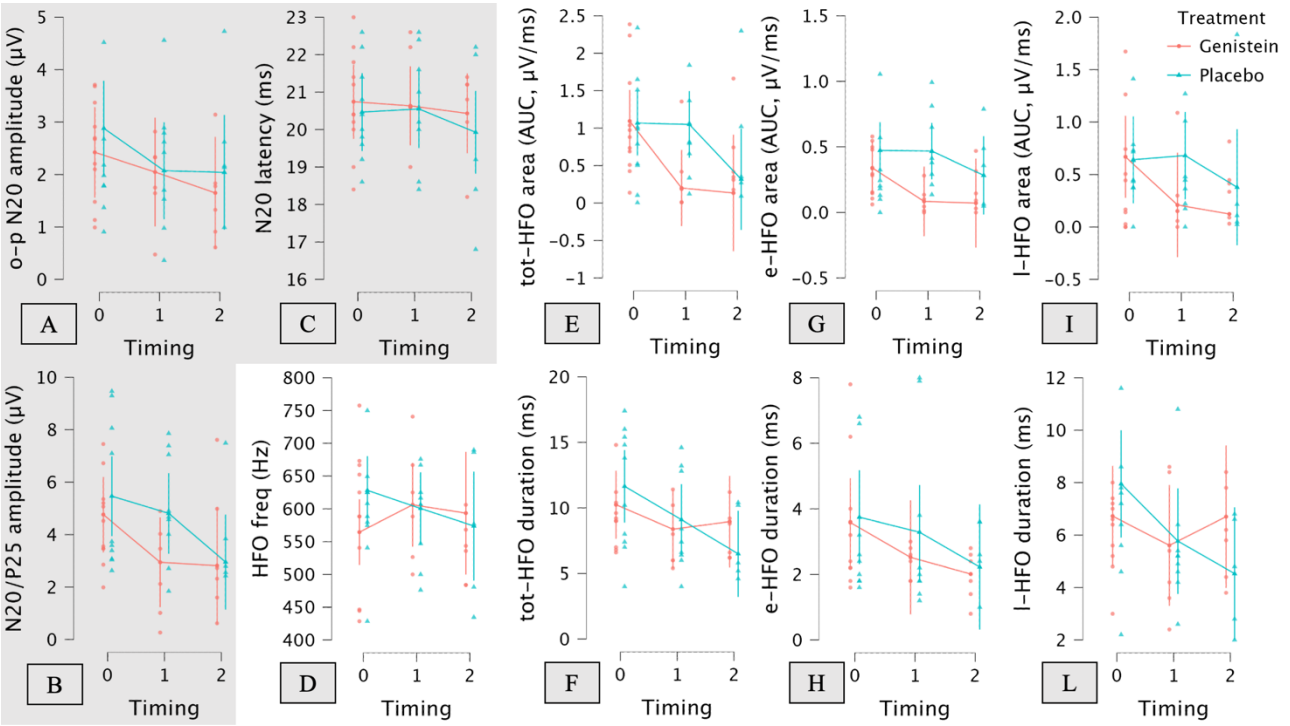

Figure 9. Longitudinal mixed-effects model–based trajectories of SEP–HFO measures.
Observed individual values (symbols) and model-based estimated marginal means with 95% confidence intervals (lines and error bars) derived from linear mixed-effects models are shown for somatosensory evoked potential (SEP) and SEP-related high-frequency oscillation (HFO) measures in the genistein and placebo groups across study visits (T0, baseline; T1, 6 months; T2, 12 months). Panels display (A) o–p N20 amplitude, (B) N20/P25 amplitude, (C) N20 latency, (D) HFO frequency, (E) total HFO area, (F) total HFO duration, (G) early HFO area, (H) early HFO duration, (I) late HFO area, and (L) late HFO duration. All models included fixed effects for treatment, time, and their interaction, together with selected covariates (education, baseline MMSE, ΔMEP, and CSF p-tau), and subject-specific random intercepts. Across measures, substantial inter-individual variability and largely overlapping confidence intervals were observed, indicating limited estimation precision; the figure is intended to illustrate longitudinal data patterns rather than provide inferential evidence. ***Abbreviations:*** *SEP, somatosensory evoked potential; HFO, high-frequency oscillations; o–p, onset-to-peak; AUC, area under the curve; CSF, cerebrospinal fluid; pTau, phosphorylated tau.*

5.4.7 Effects of treatment on cortical excitability and intracortical inhibitory/facilitatory circuits

Linear mixed-effects models were used to assess the longitudinal effects of genistein on cortical excitability and intracortical inhibitory and facilitatory circuits as measured by TMS (Figure 10). Resting motor threshold (RMT) and active motor threshold (AMT) did not show significant main effects of treatment or timing, nor significant timing-by-treatment interactions, indicating overall stability of global corticospinal excitability across the study period in both groups. Similarly, MEP amplitude at 120% RMT did not differ significantly between treatment groups; however, a timing-by-treatment interaction approached statistical significance, reflecting divergent longitudinal trajectories between groups, albeit without a clear or consistent treatment-related pattern.

Measures of sensorimotor integration and intracortical circuitry revealed a more heterogeneous profile. For SAI ratio, significant main effects of treatment ($p = 0.002$) and education ($p = 0.001$) were observed, alongside a significant effect of timing (T2, $p = 0.023$), suggesting that afferent inhibition changed over time and differed between treatment groups independently of baseline cognitive status. Post hoc comparisons of estimated marginal means demonstrated that the between-group difference was confined to the baseline time point ($p = 0.003$), while no significant differences were observed at subsequent follow-up assessments ($p > 0.05$). Thus, the treatment main effect reflects a persistent between-group offset rather than a differential treatment-induced change in SAI over time. CSF pTau showed a trend-level association with SAI ratio ($p = 0.056$).

SICI ratio did not demonstrate significant main effects of treatment or timing; however, l-HFO duration emerged as a significant covariate ($p = 0.032$), indicating an association between baseline neurophysiological properties and intracortical inhibitory tone. No significant interaction effects were observed. Similarly, ICF ratio remained stable over time, with no significant effects of treatment, timing, or their interaction, suggesting preserved facilitatory intracortical mechanisms in both groups throughout follow-up.

Overall, these findings indicate that genistein did not show evidence of treatment-induced longitudinal modulation on cortical excitability or intracortical inhibitory/facilitatory circuits during the study period.

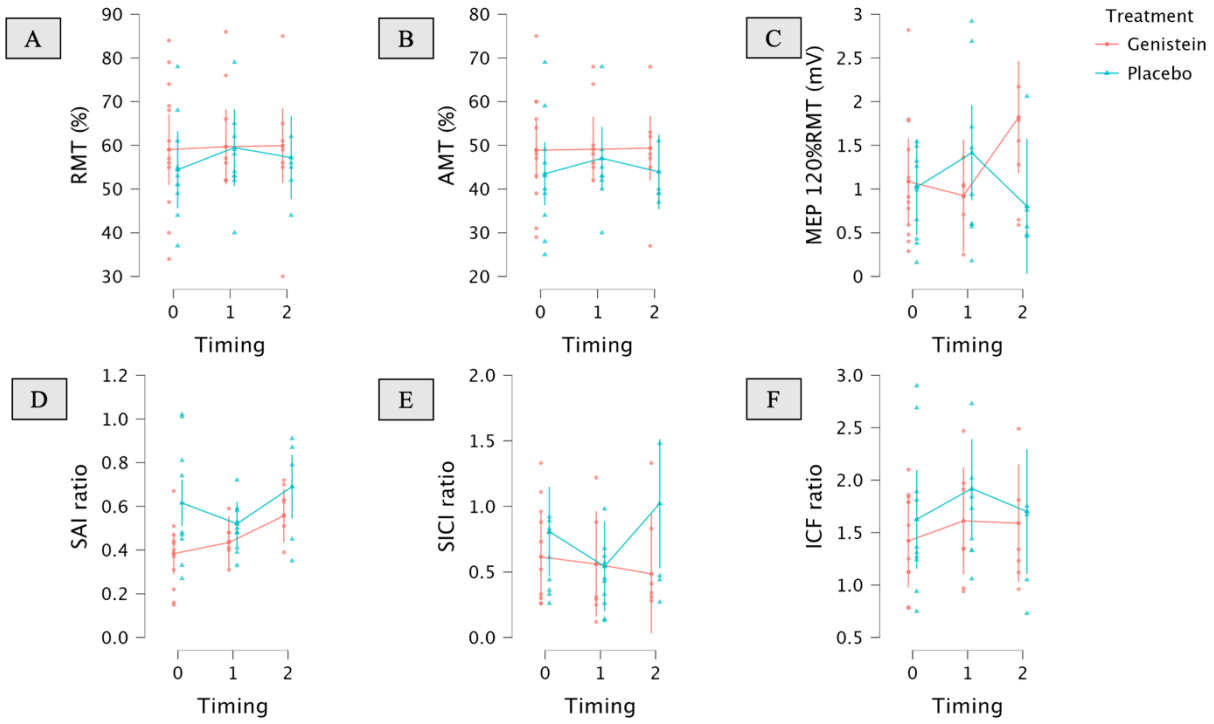

Figure 10.Longitudinal effects of genistein treatment on cortical excitability and intracortical inhibitory and facilitatory measures.

The figure shows estimated marginal means (±95% CI) derived from linear mixed-effects models for transcranial magnetic stimulation (TMS) measures across time (T0, baseline; T1, 6 months; T2, 12 months) in the genistein and placebo groups. Panels depict: (A) resting motor threshold (RMT, % of maximum stimulator output), (B) active motor threshold (AMT, %), (C) motor-evoked potential amplitude at 120% RMT (MEP, mV), (D) short-latency afferent inhibition (SAI ratio), (E) short-interval intracortical inhibition (SICI ratio), and (F) intracortical facilitation (ICF ratio). Dots represent individual observations, while lines represent model-based estimates adjusted for education, baseline MMSE, CSF pTau levels, and l-HFO duration, with participant ID included as a random effect. Higher ratios indicate reduced inhibition (for SAI and SICI) or increased facilitation (for ICF).

5.4.8 Effects of treatment on cortical plasticity

Cortical plasticity was assessed using linear mixed-effects models applied to neuromodulation-related indices, including changes in motor-evoked potential amplitude (ΔMEP), resting motor threshold (ΔRMT), and active motor threshold (ΔAMT). All models included timing and treatment as fixed factors, their interaction, and were adjusted for education, baseline MMSE score, CSF phosphorylated tau levels, and late HFO duration, with subject-specific random intercepts (Figure 11).

For ΔMEP, no significant main effect of timing or treatment, nor a significant timing-by-treatment interaction, was observed. At the parameter level, the T2 contrast was negative (Timing 2 p=0.026), suggesting a late reduction across groups; however, this pattern should be interpreted cautiously given the non-significant omnibus timing effect. Estimated marginal means showed overlapping trajectories between genistein and placebo groups at all time points, with substantial inter-individual variability.

Similarly, analyses of ΔRMT and ΔAMT did not reveal significant main effects of treatment or timing, nor any timing-by-treatment interactions. Motor threshold changes over time were modest and highly variable, with no consistent pattern differentiating the genistein and placebo groups. None of the examined covariates showed a significant association with plasticity-related outcomes.

Overall, these results indicate that genistein treatment was not associated with measurable modulation of cortical plasticity indices over the study period, and that observed changes primarily reflected non-specific temporal effects and inter-individual variability rather than treatment-related plastic responses.

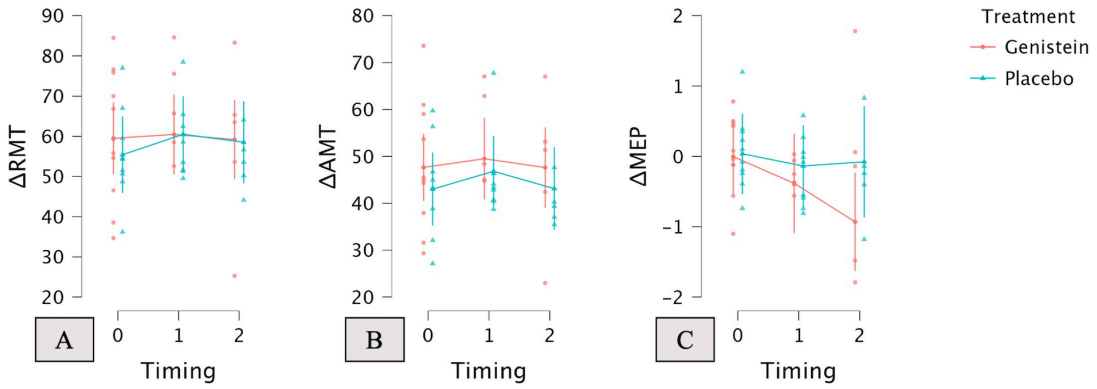

Figure 11. Effects of treatment on cortical plasticity measures.
Longitudinal trajectories of cortical plasticity indices derived from neuromodulation paradigms. Panels show estimated marginal means (±95% confidence intervals) and individual data points for (A) change in resting motor threshold (ΔRMT), (B) change in active motor threshold (ΔAMT), and (C) change in motor-evoked potential amplitude following neuromodulation (ΔMEP), across study time points (Timing 0, Timing 1, Timing 2) in participants receiving genistein (red) or placebo (blue). Estimates are derived from linear mixed-effects models including timing, treatment, and their interaction as fixed factors, with adjustment for education, baseline MMSE score, CSF phosphorylated tau levels, and late high-frequency oscillation (l-HFO) duration, and subject-specific random intercepts. No significant treatment-related or interaction effects were observed across plasticity measures.

5.5 Discussion

5.5.1 Overall summary of findings

This pilot, randomized, double-blind, placebo-controlled study explored the clinical and neurophysiological effects of chronic genistein supplementation in individuals with mild cognitive impairment due to Alzheimer's disease in a pragmatic, real-life setting.

Overall, the results provide no definitive confirmatory evidence of a treatment effect, but they do suggest a weak and partially convergent signal on global cognition, accompanied by subtle and time-dependent changes in SEP–HFO dynamics, against a background of largely stable

neuropsychological secondary outcomes and largely unchanged indices of cortical excitability and plasticity.

With respect to the primary endpoint, longitudinal mixed-effects modelling of absolute MMSE did not yield a statistically robust main effect of treatment; however, a borderline treatment-by-time contrast at T1 ($p \approx 0.051$) pointed in the direction of a less pronounced decline in the genistein group compared with placebo at follow-up. Importantly, the robustness analysis using change-from-baseline MMSE (ΔMMSE) identified a significant overall treatment effect ($p=0.017$), without evidence of a treatment-by-time interaction, consistent with an interpretation of a global between-group difference in cognitive change across follow-up rather than progressively diverging slopes. Taken together, these two model specifications converge on the same directionality—namely, a pattern compatible with relative cognitive preservation under genistein—while simultaneously highlighting the intrinsic uncertainty of estimates in a small trial.

Secondary clinical outcomes were less supportive of a treatment effect. For neuropsychiatric symptom burden (NPI), both absolute and change-score models showed no evidence of treatment-related modulation and no timing-by-treatment interaction, despite a descriptive tendency toward worsening over time in both arms. Similarly, analyses of secondary neuropsychological measures did not reveal consistent treatment effects: while some outcomes demonstrated time-dependent changes (e.g., delayed recall and digit span backward), these changes appeared independent of treatment allocation, suggesting that longitudinal cognitive dynamics in domains beyond global screening measures were driven primarily by disease progression and inter-individual variability rather than a detectable pharmacological signal.

Neurophysiological results were mixed and should be regarded as exploratory. In SEP-related endpoints, N20 latency and N20 onset-to-peak amplitude showed no significant effects of treatment, timing, or their interaction. In contrast, N20–P25 peak-to-peak amplitude displayed a clear timing effect (reductions at both follow-ups) without treatment-related divergence, indicating longitudinal change that was common to both groups.
For SEP-related high-frequency oscillations, HFO frequency did not show a treatment-related effect but was positively associated with baseline MMSE, suggesting that global cognitive status may be linked to faster oscillatory dynamics independently of treatment. Most notably, total HFO area demonstrated both a timing-related reduction and an early timing-by-treatment interaction at T1 ($p=0.038$), consistent with a transient divergence between groups after covariate adjustment. In parallel, late HFO duration showed a borderline timing-by-treatment trend at T2 ($p=0.059$).

Although neither finding constitutes robust evidence of treatment efficacy at the neurophysiological level, the temporal pattern—a more evident "signal" at T1 in total HFO area and a later borderline trend in late HFO duration—raises the possibility of a subtle, time-dependent modulation of SEP–HFO dynamics associated with genistein.

Measures derived from TMS showed, overall, no consistent indication that genistein altered cortical excitability or intracortical inhibitory/facilitatory circuits. RMT and AMT were stable, and MEP amplitude showed no convincing between-group difference despite a borderline interaction. For SAI, a statistically significant treatment main effect was observed in the mixed model, but post hoc contrasts indicated that the group difference was confined to baseline, consistent with a baseline offset rather than a treatment-induced change over time. Therefore, SAI findings do not support a causal interpretation in favour of genistein. Finally, indices of cortical plasticity (ΔMEP, ΔRMT, ΔAMT) did not show treatment-related effects or timing-by-treatment interactions, and any timing-associated changes appeared not to differentiate treatment arms.

In summary, this exploratory trial suggests: (i) a weak, directionally coherent signal compatible with relative preservation of global cognition under genistein; (ii) no detectable effect on neuropsychiatric symptoms and most secondary neuropsychological outcomes; and (iii) subtle SEP–HFO patterns that may reflect transient or non-linear modulation of sensory cortical processing, without consistent changes in TMS-based excitability or plasticity indices.

5.5.2 SEP–HFO findings: implications for sensory cortical network dynamics

Among the neurophysiological outcomes examined, SEP-related high-frequency oscillations (HFOs) emerged as the most informative markers, albeit within an exploratory framework. HFOs embedded within somatosensory evoked potentials are increasingly interpreted as indices of fast cortical processing, reflecting the synchronous activity of local neuronal assemblies and the integrity of thalamo-cortical and cortico-cortical microcircuits (Curio et al., 1994; Gobbelé et al., 2004). In this context, changes in HFO area, duration, or frequency are thought to index alterations in network efficiency, temporal coordination, or excitatory–inhibitory balance within early sensory cortex.

In the present study, total HFO area showed a significant main effect of timing, indicating a reduction over follow-up consistent with a disease-related degradation of fast oscillatory dynamics. Superimposed on this global decline, a timing-by-treatment interaction emerged at the first follow-up (T1), suggesting an early divergence between genistein and placebo groups after adjustment for

education, baseline MMSE, CSF p-tau, and ΔMEP. Although this interaction was not sustained at the final follow-up, its presence at 6-month follow-up raises the possibility of a transient modulation of fast oscillatory activity in the genistein group.

In parallel, late HFO duration displayed a borderline timing-by-treatment interaction at T2, with directionally consistent estimates. Given that late HFO components are more closely linked to intracortical processing and cortico-cortical propagation rather than purely thalamic input (Hashimoto, 2000; Ozaki and Hashimoto, 2011), this temporal dissociation—an early signal in total HFO area and a later trend in late HFO duration—may reflect a non-linear or phase-shifted modulation of sensory cortical network dynamics rather than a monotonic treatment effect.

Importantly, these SEP–HFO patterns occurred in the absence of treatment-related changes in SEP latencies or amplitudes, indicating preserved afferent conduction and gross evoked response integrity. This dissociation suggests that any putative genistein-related effect, if present, operates at the level of fast oscillatory synchronization or microcircuit dynamics rather than altering primary sensory transmission.

Finally, the positive association between baseline MMSE and HFO frequency, independent of treatment, reinforces the link between fast oscillatory dynamics and global cognitive status. This finding supports the view that SEP–HFO measures capture a neurophysiological dimension of cortical efficiency or reserve that is not redundant with standard cognitive testing and may be particularly sensitive in early disease stages.

Overall, while these findings do not provide definitive evidence of treatment efficacy, the internal coherence of the SEP–HFO pattern supports their consideration as candidate biomarkers for subtle, network-level modulation in prodromal Alzheimer's disease.

5.5.3 Toward a unifying interpretation: modest cognitive effects with subtle network-level modulation

Taken together, the clinical and neurophysiological findings of this study support a nuanced, two-level interpretation. On the clinical side, genistein supplementation was associated with a weak but directionally consistent signal compatible with relative preservation of global cognitive function, as indicated by MMSE, while failing to produce detectable effects on neuropsychiatric symptoms or domain-specific neuropsychological measures. On the neurophysiological side, exploratory SEP–HFO analyses revealed subtle, time-dependent patterns suggestive of transient modulation of

sensory cortical network dynamics, in the absence of consistent changes in TMS-based indices of cortical excitability or plasticity.

A first, more possibilistic interpretation is that genistein may exert small system-level effects on synaptic or network efficiency that are most readily captured by coarse global measures such as the MMSE and by sensitive oscillatory markers like HFOs. In this framework, the absence of effects on NPI, secondary cognitive domains, and motor TMS outcomes would not be unexpected, given the short observation window, the heterogeneity of the MCI-AD population, and the limited sensitivity of these measures to subtle or early network changes. The temporal dissociation observed within SEP–HFO measures—early modulation of total HFO area followed by a later trend in late HFO duration—would be consistent with a non-linear or compensatory network response rather than a progressive treatment-induced divergence.

At the same time, a more conservative interpretation must be considered. The small sample size, substantial inter-individual variability, missing data, and multiple testing across numerous neurophysiological endpoints limit estimation precision and increase the risk of chance findings. In this context, isolated significant or borderline contrasts—particularly when not sustained across time points—may reflect statistical fluctuation rather than a true biological effect. The lack of convergent evidence from TMS-based excitability and plasticity measures, as well as from secondary neuropsychological outcomes, further tempers causal inference.

Accordingly, the most defensible synthesis is that genistein shows a hypothesis-generating signal of modest cognitive benefit on MMSE, accompanied by exploratory SEP–HFO correlates suggestive of transient or subtle network-level modulation, but without consistent support from other clinical, neurophysiological, or biomarker measures within this dataset. These findings neither confirm nor refute a biological effect of genistein, but they delineate the domains in which such an effect—if present—may be most detectable.

5.5.4 Methodological considerations, limitations, and future neurophysiological directions

From a neurophysiological standpoint, several methodological features of this study both constrain interpretation and inform future research. First, the exploratory nature and limited sample size substantially reduce statistical power, particularly for complex mixed-effects models involving multiple covariates and interaction terms. This limitation is especially relevant for

neurophysiological outcomes, where inter-individual variability is high and effect sizes are expected to be small.

Second, the heterogeneity of neurophysiological measures—spanning SEP, HFOs, TMS-derived excitability indices, and plasticity markers—inevitably increases the multiple-testing burden and complicates interpretation. While the two-step strategy combining estimation-statistics screening with targeted LMMs mitigates some risks of overfitting, future studies would benefit from pre-specifying a smaller set of primary neurophysiological endpoints, ideally grounded in a clear mechanistic hypothesis.

Third, the dissociation observed between SEP–HFO findings and TMS-based measures of excitability and plasticity deserves specific attention. Motor TMS indices primarily probe corticospinal and motor intracortical circuits, which may be relatively insensitive to early or subtle neuromodulatory effects relevant to cognitive networks. In contrast, SEP–HFOs directly index sensory cortical microcircuit dynamics and may therefore provide greater sensitivity to early network-level changes in prodromal Alzheimer's disease. This mismatch highlights the importance of aligning neurophysiological outcomes with the hypothesised neural targets of an intervention.

Fourth, the presence of baseline offsets (e.g., SAI differences) underscores the necessity of careful modelling and cautious causal interpretation. The explicit distinction between baseline group differences and treatment-induced longitudinal changes adopted in this study represents a methodological strength and should be maintained in future work.

Looking forward, these findings suggest several directions for future trials. Larger, adequately powered studies should evaluate whether SEP–HFO measures—particularly total HFO area and late HFO duration—can serve as sensitive biomarkers of treatment-related modulation in early AD-spectrum conditions. Longitudinal designs with denser sampling may clarify whether the apparent early and late signals observed here reflect distinct phases of network adaptation. Finally, integrating SEP–HFO metrics with multimodal approaches (e.g., EEG connectivity, source-resolved oscillatory analyses, or computational modelling) may help bridge the gap between subtle neurophysiological modulation and clinical outcomes.

6. General discussion and conclusions

The present doctoral thesis investigated functional neurophysiological alterations in mild cognitive impairment due to Alzheimer's disease (MCI-AD), with the overall aim of identifying sensitive markers of early network dysfunction, short-term disease progression, and potential targets for therapeutic modulation. Across three complementary studies, we adopted a multimodal neurophysiological approach combining conventional SEP components and high-frequency SEP components (HFOs) to explore different dimensions of cortical and thalamocortical function in biomarker-confirmed MCI-AD.

Taken together, the findings of the three studies converge on a coherent framework in which early Alzheimer's disease is characterized by subtle but measurable alterations in fast network dynamics and inhibitory control, detectable before gross structural damage or overt clinical deterioration. In this context, SEP-derived HFOs emerged as a particularly sensitive and consistent neurophysiological marker, linking cross-sectional disease-related alterations (**Study 1**), short-term clinical progression (**Study 2**), and exploratory treatment-related modulation (**Study 3**).

6.1 Early thalamocortical dysfunction as a core feature of prodromal AD

Study 1 demonstrated that patients with biomarker-confirmed MCI-AD exhibit marked alterations in SEP-related HFOs despite preserved conventional SEP parameters such as N20 latency and amplitude. This dissociation suggests that early Alzheimer's disease does not primarily impair afferent somatosensory conduction, but rather disrupts the temporal organization and persistence of fast oscillatory activity within thalamocortical and intracortical circuits.

The prolongation of both early and late HFO components points toward a loss of temporal precision and altered synchronization, consistent with early synaptic dysfunction. Early HFOs, reflecting presynaptic thalamocortical input and fast excitatory cortical processing, and late HFOs, indexing cortico-cortical integration, were both affected, indicating that thalamic drive and cortical network integration are simultaneously compromised at the prodromal stage (Ozaki and Hashimoto, 2011). These findings align with neuropathological and neuroimaging evidence implicating early thalamic involvement in Alzheimer's disease and support the conceptualization of AD as a disorder of large-scale network dynamics rather than focal regional pathology (Lo et al., 2010).

6.2 SEP–HFO dynamics predict short-term clinical progression

Building on these cross-sectional findings, **Study 2** demonstrated that SEP–HFO measures are not merely epiphenomenal but carry prognostic significance.

In particular, baseline prolongation of early HFO duration independently predicted cognitive decline over a 6-month follow-up period, with a graded increase from healthy subjects to MCI-AD non-progressors and MCI-AD progressors.
This stepwise pattern strongly suggests that e-HFO duration reflects progressive deterioration of thalamocortical efficiency and network timing. The predictive value of e-HFO duration remained significant in multivariate models incorporating demographic and neurophysiological covariates, underscoring its robustness as a functional marker of disease trajectory. Importantly, this prognostic information was obtained independently of cerebrospinal fluid biomarkers, highlighting the complementary role of neurophysiology in capturing dynamic aspects of network dysfunction that are not accessible through static molecular measures.

In terms of underlying neural mechanisms, prolonged early HFOs likely reflect temporal dispersion and maladaptive hypersynchrony within thalamocortical circuits, phenomena implicated in other neuropsychiatric and neurodegenerative disorders characterized by impaired inhibitory control and altered oscillatory coordination (Poulet et al., 2012; Uhlhaas and Singer, 2010). In Alzheimer's disease, such alterations may represent an early electrophysiological signature of network vulnerability preceding overt neuronal loss.

6.3 Inhibitory dysfunction and network instability

Across **Studies 1 and 2**, alterations in intracortical inhibition, as indexed by short-interval intracortical inhibition (SICI), further supported the notion of early network imbalance in MCI-AD. Although SICI did not retain independent predictive value in multivariate models, its association with disease status and progression risk at the univariate level is consistent with a broader literature describing reduced GABAergic inhibition in Alzheimer's disease (Di Lazzaro et al., 2004; Ferreri et al., 2003; Nardone et al., 2014).

The convergence of prolonged HFO duration and reduced inhibitory tone suggests a model in which early synaptic dysfunction leads to impaired temporal regulation of cortical activity. In this framework, inhibitory interneurons play a critical role in shaping oscillatory timing and preventing excessive or prolonged synchronization. Their dysfunction may therefore contribute to the abnormal persistence of high-frequency oscillatory activity observed in MCI-AD, driving network instability and accelerating cognitive decline.
This interpretation is further supported by converging experimental evidence indicating that early Alzheimer's disease is characterized by network hyperexcitability driven by impaired inhibitory

control and altered fast oscillatory activity, involving parvalbumin interneurons and dopaminergic modulation of hippocampal circuits (Spoleti et al., 2024).

6.4 Neurophysiological markers as tools for prognostic stratification

One of the key implications of this work lies in the potential clinical utility of neurophysiological markers for prognostic stratification in MCI-AD.

Study 2 provides proof of principle that functional measures derived from conventional and high-frequency SEP components can identify patients at higher risk of short-term progression, with reasonable discriminative performance.

In the current therapeutic landscape, characterized by the emergence of disease-modifying treatments with non-negligible risks (van Dyck et al., 2023; Mintun et al., 2021), the ability to identify patients most likely to progress in the near term is of paramount importance.

Neurophysiological biomarkers may contribute to this goal by offering repeatable, low-cost, and dynamic measures of network function that complement established molecular and imaging markers.

6.5 Genistein as a probe of network-level modulation

Study 3 extended this framework by exploring whether chronic genistein supplementation could modulate cognitive outcomes and neurophysiological markers in MCI-AD.

While the trial did not provide definitive evidence of treatment efficacy, a weak but directionally coherent signal emerged, compatible with relative preservation of global cognition as measured by MMSE.

At the neurophysiological level, exploratory analyses revealed subtle, time-dependent patterns in high-frequency SEP components, including an early divergence in total HFO area and a later trend in late HFO duration.

Although these effects were not robust or sustained, their internal coherence and alignment with the neurophysiological markers identified in **Studies 1 and 2** suggest that HFOs may represent a sensitive readout of subtle network-level modulation.

Importantly, the absence of consistent effects on TMS-derived measures of cortical excitability and plasticity highlights the specificity of high-frequency SEP components for sensory cortical microcircuits and underscores the need to align neurophysiological endpoints with hypothesized mechanisms of action.

6.6 Limitations and future directions

Several limitations must be acknowledged. Sample sizes were modest, particularly in the randomized trial, limiting statistical power and estimation precision. The exploratory nature of multiple neurophysiological endpoints increases the risk of chance findings, and pharmacological treatments may have influenced some TMS measures.
Nevertheless, the use of biomarker-confirmed MCI-AD cohorts, longitudinal designs, and advanced neurophysiological analyses represent major strengths of this work.

Future studies should aim to validate high-frequency SEP measures in larger, independent cohorts and to integrate them with other functional modalities such as EEG connectivity and functional brain MRI.

Taken together, the results of this thesis indicate that SEP-derived HFOs capture early alterations in network dynamics that are clinically relevant in prodromal Alzheimer's disease, supporting their potential role as functional biomarkers for prognostic stratification and for the assessment of target-specific effects in early-stage intervention studies.

References

Aggleton JP, Pralus A, Nelson AJD, Hornberger M. Thalamic pathology and memory loss in early Alzheimer's disease: moving the focus from the medial temporal lobe to Papez circuit. Brain 2016;139:1877–90. https://doi.org/10.1093/brain/aww083.

Albert MS, DeKosky ST, Dickson D, Dubois B, Feldman HH, Fox NC, et al. The diagnosis of mild cognitive impairment due to Alzheimer's disease: recommendations from the National Institute on Aging-Alzheimer's Association workgroups on diagnostic guidelines for Alzheimer's disease. Alzheimers Dement 2011;7:270–9. https://doi.org/10.1016/j.jalz.2011.03.008.

Andreasson U, Perret-Liaudet A, van Waalwijk van Doorn LJC, Blennow K, Chiasserini D, Engelborghs S, et al. A Practical Guide to Immunoassay Method Validation. Front Neurol 2015;6:179. https://doi.org/10.3389/fneur.2015.00179.

Babiloni C, Del Percio C, Lizio R, Marzano N, Infarinato F, Soricelli A, et al. Cortical sources of resting state electroencephalographic alpha rhythms deteriorate across time in subjects with amnesic mild cognitive impairment. Neurobiol Aging 2014;35:130–42. https://doi.org/10.1016/j.neurobiolaging.2013.06.019.

Baddeley A. Working memory. Science 1992;255:556–9. https://doi.org/10.1126/science.1736359.

Bagheri M, Joghataei M-T, Mohseni S, Roghani M. Genistein ameliorates learning and memory deficits in amyloid β(1–40) rat model of Alzheimer's disease. Neurobiology of Learning and Memory 2011;95:270–6. https://doi.org/10.1016/j.nlm.2010.12.001.

Benavides F, Chen R, Jo HJ. Enhanced cortical facilitation after intermittent theta burst stimulation with increased stimulation intensity. Clinical Neurophysiology 2025;180:2111382. https://doi.org/10.1016/j.clinph.2025.2111382.

Bozzali M, Giulietti G, Basile B, Serra L, Spanò B, Perri R, et al. Damage to the cingulum contributes to alzheimer's disease pathophysiology by deafferentation mechanism. Hum Brain Mapp 2011;33:1295–308. https://doi.org/10.1002/hbm.21287.

Braak H, Braak E. Alzheimer's disease affects limbic nuclei of the thalamus. Acta Neuropathol 1991;81:261–8. https://doi.org/10.1007/BF00305867.

Braak H, Del Tredici K. The pathological process underlying Alzheimer's disease in individuals under thirty. Acta Neuropathol 2011;121:171–81. https://doi.org/10.1007/s00401-010-0789-4.

Budd Haeberlein S, Aisen PS, Barkhof F, Chalkias S, Chen T, Cohen S, et al. Two Randomized Phase 3 Studies of Aducanumab in Early Alzheimer's Disease. J Prev Alzheimers Dis 2022;9:197–210. https://doi.org/10.14283/jpad.2022.30.

Capone F, Motolese F, Rossi M, Musumeci G, Insola A, Di Lazzaro V. Thalamo-cortical dysfunction contributes to fatigability in multiple sclerosis patients: A neurophysiological study. Mult Scler Relat Disord 2019;39:101897. https://doi.org/10.1016/j.msard.2019.101897.

Chan NK, Gerretsen P, Chakravarty MM, Blumberger DM, Caravaggio F, Brown E, et al. Structural Brain Differences Between Cognitively Impaired Patients With and Without Apathy. Am J Geriatr Psychiatry 2021;29:319–32. https://doi.org/10.1016/j.jagp.2020.12.008.

Chen X, Wu Y, Gu J, Liang P, Shen M, Xi J, et al. Anti-invasive effect and pharmacological mechanism of genistein against colorectal cancer. Biofactors 2020;46:620–8. https://doi.org/10.1002/biof.1627.

Cordella A, Krashia P, Nobili A, Pignataro A, La Barbera L, Viscomi MT, et al. Dopamine loss alters the hippocampus-nucleus accumbens synaptic transmission in the Tg2576 mouse model of Alzheimer's disease. Neurobiol Dis 2018;116:142–54. https://doi.org/10.1016/j.nbd.2018.05.006.

Cristofalo A, Cascini S, Cesaroni G, Trappolini E, Agabiti N, Bargagli AM. Educational disparities in dementia incidence and healthcare utilization: evidence from a cohort study in Italy. Soc Sci Med 2025;380:118233. https://doi.org/10.1016/j.socscimed.2025.118233.

Cummings JL. The Neuropsychiatric Inventory: assessing psychopathology in dementia patients. Neurology 1997;48:S10-16. https://doi.org/10.1212/wnl.48.5_suppl_6.10s.

Cummings JL, Mega M, Gray K, Rosenberg-Thompson S, Carusi DA, Gornbein J. The Neuropsychiatric Inventory: comprehensive assessment of psychopathology in dementia. Neurology 1994;44:2308–14. https://doi.org/10.1212/wnl.44.12.2308.

Curio G, Mackert BM, Burghoff M, Koetitz R, Abraham-Fuchs K, Härer W. Localization of evoked neuromagnetic 600 Hz activity in the cerebral somatosensory system. Electroencephalogr Clin Neurophysiol 1994;91:483–7. https://doi.org/10.1016/0013-4694(94)90169-4.

Di Lazzaro V, Oliviero A, Pilato F, Saturno E, Dileone M, Marra C, et al. Motor cortex hyperexcitability to transcranial magnetic stimulation in Alzheimer's disease. J Neurol Neurosurg Psychiatry 2004;75:555–9. https://doi.org/10.1136/jnnp.2003.018127.

Di Lazzaro V, Oliviero A, Profice P, Pennisi MA, Di Giovanni S, Zito G, et al. Muscarinic receptor blockade has differential effects on the excitability of intracortical circuits in the human motor cortex. Exp Brain Res 2000;135:455–61. https://doi.org/10.1007/s002210000543.

Di Lazzaro V, Oliviero A, Tonali PA, Marra C, Daniele A, Profice P, et al. Noninvasive in vivo assessment of cholinergic cortical circuits in AD using transcranial magnetic stimulation. Neurology 2002;59:392–7. https://doi.org/10.1212/wnl.59.3.392.

Di Lazzaro V, Profice P, Pilato F, Capone F, Ranieri F, Pasqualetti P, et al. Motor cortex plasticity predicts recovery in acute stroke. Cereb Cortex 2010;20:1523–8. https://doi.org/10.1093/cercor/bhp216.

Di Lazzaro V, Ziemann U. The contribution of transcranial magnetic stimulation in the functional evaluation of microcircuits in human motor cortex. Front Neural Circuits 2013;7:18. https://doi.org/10.3389/fncir.2013.00018.

Diamond BJ, DeLuca J. Rey-Osterrieth Complex Figure Test performance following anterior communicating artery aneurysm. Archives of Clinical Neuropsychology 1996;11:21–8. https://doi.org/10.1016/0887-6177(95)00001-1.

Dubois B, Villain N, Schneider L, Fox N, Campbell N, Galasko D, et al. Alzheimer Disease as a Clinical-Biological Construct-An International Working Group Recommendation. JAMA Neurol 2024;81:1304–11. https://doi.org/10.1001/jamaneurol.2024.3770.

van Dyck CH, Swanson CJ, Aisen P, Bateman RJ, Chen C, Gee M, et al. Lecanemab in Early Alzheimer's Disease. N Engl J Med 2023;388:9–21. https://doi.org/10.1056/NEJMoa2212948.

Ferguson SA, Flynn KM, Delclos KB, Newbold RR, Gough BJ. Effects of lifelong dietary exposure to genistein or nonylphenol on amphetamine-stimulated striatal dopamine release in male and female rats. Neurotoxicology and Teratology 2002;24:37–45. https://doi.org/10.1016/S0892-0362(01)00193-3.

Ferreri F, Pauri F, Pasqualetti P, Fini R, Dal Forno G, Rossini PM. Motor cortex excitability in Alzheimer's disease: a transcranial magnetic stimulation study. Ann Neurol 2003;53:102–8. https://doi.org/10.1002/ana.10416.

File SE, Jarrett N, Fluck E, Duffy R, Casey K, Wiseman H. Eating soya improves human memory. Psychopharmacology (Berl) 2001;157:430–6. https://doi.org/10.1007/s002130100845.

Folstein MF, Folstein SE, McHugh PR. “Mini-mental state”. A practical method for grading the cognitive state of patients for the clinician. J Psychiatr Res 1975;12:189–98. https://doi.org/10.1016/0022-3956(75)90026-6.

Forsberg A, Engler H, Almkvist O, Blomquist G, Hagman G, Wall A, et al. PET imaging of amyloid deposition in patients with mild cognitive impairment. Neurobiol Aging 2008;29:1456–65. https://doi.org/10.1016/j.neurobiolaging.2007.03.029.

Freitas C, Mondragón-Llorca H, Pascual-Leone A. Noninvasive brain stimulation in Alzheimer’s disease: Systematic review and perspectives for the future. Experimental Gerontology 2011;46:611–27. https://doi.org/10.1016/j.exger.2011.04.001.

GBD 2019 Dementia Forecasting Collaborators. Estimation of the global prevalence of dementia in 2019 and forecasted prevalence in 2050: an analysis for the Global Burden of Disease Study 2019. Lancet Public Health 2022;7:e105–25. https://doi.org/10.1016/S2468-2667(21)00249-8.

Geda YE, Roberts RO, Knopman DS, Petersen RC, Christianson TJH, Pankratz VS, et al. The Prevalence of Neuropsychiatric Symptoms in Mild Cognitive Impairment and Normal Cognitive Aging: A Population-Based Study. Arch Gen Psychiatry 2008;65:1193–8. https://doi.org/10.1001/archpsyc.65.10.1193.

Gili T, Cercignani M, Serra L, Perri R, Giove F, Maraviglia B, et al. Regional brain atrophy and functional disconnection across Alzheimer’s disease evolution. J Neurol Neurosurg Psychiatry 2011;82:58–66. https://doi.org/10.1136/jnnp.2009.199935.

Gloria Y, Ceyzériat K, Tsartsalis S, Millet P, Tournier BB. Dopaminergic dysfunction in the 3xTg-AD mice model of Alzheimer’s disease. Sci Rep 2021;11:19412. https://doi.org/10.1038/s41598-021-99025-1.

Gobbelé R, Waberski TD, Simon H, Peters E, Klostermann F, Curio G, et al. Different origins of low- and high-frequency components (600 Hz) of human somatosensory evoked potentials. Clin Neurophysiol 2004;115:927–37. https://doi.org/10.1016/j.clinph.2003.11.009.

Guerra A, Assenza F, Bressi F, Scrascia F, Del Duca M, Ursini F, et al. Transcranial magnetic stimulation studies in Alzheimer’s disease. Int J Alzheimers Dis 2011;2011:263817. https://doi.org/10.4061/2011/263817.

Gustavsson A, Norton N, Fast T, Frölich L, Georges J, Holzapfel D, et al. Global estimates on the number of persons across the Alzheimer's disease continuum. Alzheimers Dement 2023;19:658–70. https://doi.org/10.1002/alz.12694.

Hampel H, Mesulam M-M, Cuello AC, Farlow MR, Giacobini E, Grossberg GT, et al. The cholinergic system in the pathophysiology and treatment of Alzheimer's disease. Brain 2018;141:1917–33. https://doi.org/10.1093/brain/awy132.

Hashimoto I. High-frequency oscillations of somatosensory evoked potentials and fields. J Clin Neurophysiol 2000;17:309–20. https://doi.org/10.1097/00004691-200005000-00008.

Hölttä EH, Laakkonen M-L, Laurila JV, Strandberg TE, Tilvis RS, Pitkälä KH. Apathy: prevalence, associated factors, and prognostic value among frail, older inpatients. J Am Med Dir Assoc 2012;13:541–5. https://doi.org/10.1016/j.jamda.2012.04.005.

Iaccarino L, Sala A, Caminiti SP, Presotto L, Perani D, Alzheimer's Disease Neuroimaging Initiative. In vivo MRI Structural and PET Metabolic Connectivity Study of Dopamine Pathways in Alzheimer's Disease. J Alzheimers Dis 2020;75:1003–16. https://doi.org/10.3233/JAD-190954.

Insola A, Di Lazzaro V, Assenza G. Cortical inhibitory dysfunction in epilepsia partialis continua: A high frequency oscillation somatosensory evoked potential study. Clin Neurophysiol 2019;130:439–44. https://doi.org/10.1016/j.clinph.2019.01.005.

Jack CR, Andrews JS, Beach TG, Buracchio T, Dunn B, Graf A, et al. Revised criteria for diagnosis and staging of Alzheimer's disease: Alzheimer's Association Workgroup. Alzheimers Dement 2024;20:5143–69. https://doi.org/10.1002/alz.13859.

Jack CR, Bennett DA, Blennow K, Carrillo MC, Dunn B, Haeberlein SB, et al. NIA-AA Research Framework: Toward a biological definition of Alzheimer's disease. Alzheimers Dement 2018;14:535–62. https://doi.org/10.1016/j.jalz.2018.02.018.

Jack CR, Wiste HJ, Vemuri P, Weigand SD, Senjem ML, Zeng G, et al. Brain beta-amyloid measures and magnetic resonance imaging atrophy both predict time-to-progression from mild cognitive impairment to Alzheimer's disease. Brain 2010;133:3336–48. https://doi.org/10.1093/brain/awq277.

Jørgensen M, Vendelbo B, Skakkebaek NE, Leffers H. Assaying estrogenicity by quantitating the expression levels of endogenous estrogen-regulated genes. Environ Health Perspect 2000;108:403–12. https://doi.org/10.1289/ehp.108-1638061.

Ju YH, Allred CD, Allred KF, Karko KL, Doerge DR, Helferich WG. Physiological Concentrations of Dietary Genistein Dose-Dependently Stimulate Growth of Estrogen-Dependent Human Breast Cancer (MCF-7) Tumors Implanted in Athymic Nude Mice. The Journal of Nutrition 2001;131:2957–62. https://doi.org/10.1093/jn/131.11.2957.

Kaufman PB, Duke JA, Brielmann H, Boik J, Hoyt JE. A comparative survey of leguminous plants as sources of the isoflavones, genistein and daidzein: implications for human nutrition and health. J Altern Complement Med 1997;3:7–12. https://doi.org/10.1089/acm.1997.3.7.

Kerrigan TL, Randall AD. A New Player in the "Synaptopathy" of Alzheimer's Disease – Arc/Arg 3.1. Front Neurol 2013;4:9. https://doi.org/10.3389/fneur.2013.00009.

Kim DH, Jung W-S, Kim ME, Lee H-W, Youn H-Y, Seon JK, et al. Genistein inhibits pro-inflammatory cytokines in human mast cell activation through the inhibition of the ERK pathway. Int J Mol Med 2014;34:1669–74. https://doi.org/10.3892/ijmm.2014.1956.

Kim D-J, Seok S-H, Baek M-W, Lee H-Y, Na Y-R, Park S-H, et al. Developmental toxicity and brain aromatase induction by high genistein concentrations in zebrafish embryos. Toxicol Mech Methods 2009;19:251–6. https://doi.org/10.1080/15376510802563330.

Krashia P, Nobili A, D'Amelio M. Unifying Hypothesis of Dopamine Neuron Loss in Neurodegenerative Diseases: Focusing on Alzheimer's Disease. Front Mol Neurosci 2019;12:123. https://doi.org/10.3389/fnmol.2019.00123.

Krashia P, Spoleti E, D'Amelio M. The VTA dopaminergic system as diagnostic and therapeutical target for Alzheimer's disease. Front Psychiatry 2022;13:1039725. https://doi.org/10.3389/fpsyt.2022.1039725.

Kujirai T, Caramia MD, Rothwell JC, Day BL, Thompson PD, Ferbert A, et al. Corticocortical inhibition in human motor cortex. J Physiol 1993;471:501–19. https://doi.org/10.1113/jphysiol.1993.sp019912.

Lanctôt KL, Agüera-Ortiz L, Brodaty H, Francis PT, Geda YE, Ismail Z, et al. Apathy associated with neurocognitive disorders: Recent progress and future directions. Alzheimers Dement 2017;13:84–100. https://doi.org/10.1016/j.jalz.2016.05.008.

Le Heron C, Apps M a. J, Husain M. The anatomy of apathy: A neurocognitive framework for amotivated behaviour. Neuropsychologia 2018;118:54–67. https://doi.org/10.1016/j.neuropsychologia.2017.07.003.

Lezak MD, Howieson DB, Bigler ED, Tranel D. Neuropsychological assessment, 5th ed. New York, NY, US: Oxford University Press; 2012.

van der Linde RM, Matthews FE, Dening T, Brayne C. Patterns and persistence of behavioural and psychological symptoms in those with cognitive impairment: the importance of apathy. Int J Geriatr Psychiatry 2017;32:306–15. https://doi.org/10.1002/gps.4464.

Liu L-X, Chen W-F, Xie J-X, Wong M-S. Neuroprotective effects of genistein on dopaminergic neurons in the mice model of Parkinson's disease. Neuroscience Research 2008;60:156–61. https://doi.org/10.1016/j.neures.2007.10.005.

Lo C-Y, Wang P-N, Chou K-H, Wang J, He Y, Lin C-P. Diffusion tensor tractography reveals abnormal topological organization in structural cortical networks in Alzheimer's disease. J Neurosci 2010;30:16876–85. https://doi.org/10.1523/JNEUROSCI.4136-10.2010.

Low A, Mak E, Malpetti M, Chouliaras L, Nicastro N, Su L, et al. Asymmetrical atrophy of thalamic subnuclei in Alzheimer's disease and amyloid-positive mild cognitive impairment is associated with key clinical features. Alzheimer's & Dementia: Diagnosis, Assessment & Disease Monitoring 2019;11:690–9. https://doi.org/10.1016/j.dadm.2019.08.001.

Lyketsos CG, Carrillo MC, Ryan JM, Khachaturian AS, Trzepacz P, Amatniek J, et al. Neuropsychiatric symptoms in Alzheimer's disease. Alzheimers Dement 2011;7:532–9. https://doi.org/10.1016/j.jalz.2011.05.2410.

Ma L. Depression, Anxiety, and Apathy in Mild Cognitive Impairment: Current Perspectives. Front Aging Neurosci 2020;12:9. https://doi.org/10.3389/fnagi.2020.00009.

Manca R, Valera-Bermejo JM, Venneri A, Alzheimer's Disease Neuroimaging Initiative. Accelerated atrophy in dopaminergic targets and medial temporo-parietal regions precedes the onset

of delusions in patients with Alzheimer's disease. Eur Arch Psychiatry Clin Neurosci 2023;273:229–41. https://doi.org/10.1007/s00406-022-01417-5.

Marini H, Minutoli L, Polito F, Bitto A, Altavilla D, Atteritano M, et al. Effects of the phytoestrogen genistein on bone metabolism in osteopenic postmenopausal women: a randomized trial. Ann Intern Med 2007;146:839–47. https://doi.org/10.7326/0003-4819-146-12-200706190-00005.

Markiewicz L, Garey J, Adlercreutz H, Gurpide E. *In vitro* bioassays of non-steroidal phytoestrogens. The Journal of Steroid Biochemistry and Molecular Biology 1993;45:399–405. https://doi.org/10.1016/0960-0760(93)90009-L.

Miller DS, Robert P, Ereshefsky L, Adler L, Bateman D, Cummings J, et al. Diagnostic criteria for apathy in neurocognitive disorders. Alzheimers Dement 2021;17:1892–904. https://doi.org/10.1002/alz.12358.

Mintun MA, Lo AC, Duggan Evans C, Wessels AM, Ardayfio PA, Andersen SW, et al. Donanemab in Early Alzheimer's Disease. N Engl J Med 2021;384:1691–704. https://doi.org/10.1056/NEJMoa2100708.

Miodini P, Fioravanti L, Fronzo GD, Cappelletti V. The two phyto-oestrogens genistein and quercetin exert different effects on oestrogen receptor function. Br J Cancer 1999;80:1150–5. https://doi.org/10.1038/sj.bjc.6690479.

Mj L, A S-S, I S, V O, A N, N LB, et al. Clinical validation of the Lumipulse G cerebrospinal fluid assays for routine diagnosis of Alzheimer's disease. Alzheimer's Research & Therapy 2019;11. https://doi.org/10.1186/s13195-019-0550-8.

Moreno-Castilla P, Rodriguez-Duran LF, Guzman-Ramos K, Barcenas-Femat A, Escobar ML, Bermudez-Rattoni F. Dopaminergic neurotransmission dysfunction induced by amyloid-β transforms cortical long-term potentiation into long-term depression and produces memory impairment. Neurobiol Aging 2016;41:187–99. https://doi.org/10.1016/j.neurobiolaging.2016.02.021.

Moretti DV. Theta and alpha EEG frequency interplay in subjects with mild cognitive impairment: evidence from EEG, MRI, and SPECT brain modifications. Front Aging Neurosci 2015;7:31. https://doi.org/10.3389/fnagi.2015.00031.

Mortby ME, Adler L, Agüera-Ortiz L, Bateman DR, Brodaty H, Cantillon M, et al. Apathy as a Treatment Target in Alzheimer's Disease: Implications for Clinical Trials. Am J Geriatr Psychiatry 2022;30:119–47. https://doi.org/10.1016/j.jagp.2021.06.016.

Mortby ME, Burns R, Eramudugolla R, Ismail Z, Anstey KJ. Neuropsychiatric Symptoms and Cognitive Impairment: Understanding the Importance of Co-Morbid Symptoms. J Alzheimers Dis 2017;59:141–53. https://doi.org/10.3233/JAD-170050.

Mortby ME, Ismail Z, Anstey KJ. Prevalence estimates of mild behavioral impairment in a population-based sample of pre-dementia states and cognitively healthy older adults. Int Psychogeriatr 2018;30:221–32. https://doi.org/10.1017/S1041610217001909.

Motolese F, Rossi M, Capone F, Cruciani A, Musumeci G, Manzo M, et al. High-frequency oscillations-based precise temporal resolution of short latency afferent inhibition in the human brain. Clin Neurophysiol 2022;144:135–41. https://doi.org/10.1016/j.clinph.2022.09.006.

Nardone R, Tezzon F, Höller Y, Golaszewski S, Trinka E, Brigo F. Transcranial magnetic stimulation (TMS)/repetitive TMS in mild cognitive impairment and Alzheimer's disease. Acta Neurol Scand 2014;129:351–66. https://doi.org/10.1111/ane.12223.

Nijsten JMH, Leontjevas R, Pat-El R, Smalbrugge M, Koopmans RTCM, Gerritsen DL. Apathy: Risk Factor for Mortality in Nursing Home Patients. J Am Geriatr Soc 2017;65:2182–9. https://doi.org/10.1111/jgs.15007.

Nobili A, Latagliata EC, Viscomi MT, Cavallucci V, Cutuli D, Giacovazzo G, et al. Dopamine neuronal loss contributes to memory and reward dysfunction in a model of Alzheimer's disease. Nat Commun 2017;8:14727. https://doi.org/10.1038/ncomms14727.

Norata D, Musumeci G, Todisco A, Cruciani A, Motolese F, Capone F, et al. Bilateral median nerve stimulation and High-Frequency Oscillations unveil interhemispheric inhibition of primary sensory cortex. Clin Neurophysiol 2024;165:154–65. https://doi.org/10.1016/j.clinph.2024.06.011.

Ozaki I, Hashimoto I. Exploring the physiology and function of high-frequency oscillations (HFOs) from the somatosensory cortex. Clin Neurophysiol 2011;122:1908–23. https://doi.org/10.1016/j.clinph.2011.05.023.

Pan Y, Anthony M, Watson S, Clarkson TB. Soy Phytoestrogens Improve Radial Arm Maze Performance in Ovariectomized Retired Breeder Rats and Do Not Attenuate Benefits of 17β-Estradiol Treatment. Menopause 2000;7:230.

Peters ME, Schwartz S, Han D, Rabins PV, Steinberg M, Tschanz JT, et al. Neuropsychiatric symptoms as predictors of progression to severe Alzheimer's dementia and death: The Cache County Dementia Progression Study. Am J Psychiatry 2015;172:460–5. https://doi.org/10.1176/appi.ajp.2014.14040480.

Poulet JFA, Fernandez LMJ, Crochet S, Petersen CCH. Thalamic control of cortical states. Nat Neurosci 2012;15:370–2. https://doi.org/10.1038/nn.3035.

Rey A. L'examen clinique en psychologie. Presses universitaires de France; 1964.

Rey A. L'examen psychologique dans les cas d'encéphalopathie traumatique: (Les problèmes). Librairie Naville & Cie; 1941.

Rossini PM, Barker AT, Berardelli A, Caramia MD, Caruso G, Cracco RQ, et al. Non-invasive electrical and magnetic stimulation of the brain, spinal cord and roots: basic principles and procedures for routine clinical application. Report of an IFCN committee. Electroencephalogr Clin Neurophysiol 1994;91:79–92. https://doi.org/10.1016/0013-4694(94)90029-9.

Rossini PM, Rossi S. Transcranial magnetic stimulation: diagnostic, therapeutic, and research potential. Neurology 2007;68:484–8. https://doi.org/10.1212/01.wnl.0000250268.13789.b2.

Ruiz-Larrea MB, Mohan AR, Paganga G, Miller NJ, Bolwell GP, Rice-Evans CA. Antioxidant Activity of Phytoestrogenic Isoflavones. Free Radical Research 1997;26:63–70. https://doi.org/10.3109/10715769709097785.

Schmidt M. Rey Auditory Verbal Learning Test: RAVLT : a Handbook. Western Psychological Services; 1996.

Serra L, D'Amelio M, Di Domenico C, Dipasquale O, Marra C, Mercuri NB, et al. In vivo mapping of brainstem nuclei functional connectivity disruption in Alzheimer's disease. Neurobiol Aging 2018;72:72–82. https://doi.org/10.1016/j.neurobiolaging.2018.08.012.

Shankar AK, Javali M, Mehta A, Pradeep R, Mahale R, Acharya P, et al. Role of High Frequency Oscillations of Somatosensory Evoked Potentials in Deciphering Pathophysiology of Migraine. J Neurosci Rural Pract 2021;12:12–5. https://doi.org/10.1055/s-0040-1716793.

Sherman C, Liu CS, Herrmann N, Lanctôt KL. Prevalence, neurobiology, and treatments for apathy in prodromal dementia. Int Psychogeriatr 2018;30:177–84. https://doi.org/10.1017/S1041610217000527.

Shin M-S, Park S-Y, Park S-R, Seol S-H, Kwon JS. Clinical and empirical applications of the Rey-Osterrieth Complex Figure Test. Nat Protoc 2006;1:892–9. https://doi.org/10.1038/nprot.2006.115.

Si H, Liu D. Phytochemical genistein in the regulation of vascular function: new insights. Curr Med Chem 2007;14:2581–9. https://doi.org/10.2174/092986707782023325.

Spoleti E, La Barbera L, Cauzzi E, De Paolis ML, Saba L, Marino R, et al. Dopamine neuron degeneration in the Ventral Tegmental Area causes hippocampal hyperexcitability in experimental Alzheimer's Disease. Mol Psychiatry 2024;29:1265–80. https://doi.org/10.1038/s41380-024-02408-9.

Sturmey P, Gatherer A, Ghadiali E, Hallett S, Searle Y. The Wechsler Adult Intelligence Scale—Revised (WAIS-R): factor structure in a British, neurologically impaired population. Personality and Individual Differences 1993;14:255–7. https://doi.org/10.1016/0191-8869(93)90198-C.

Taber KH, Wen C, Khan A, Hurley RA. The limbic thalamus. J Neuropsychiatry Clin Neurosci 2004;16:127–32. https://doi.org/10.1176/jnp.16.2.127.

Thangavel P, Puga-Olguín A, Rodríguez-Landa JF, Zepeda RC. Genistein as Potential Therapeutic Candidate for Menopausal Symptoms and Other Related Diseases. Molecules 2019;24:3892. https://doi.org/10.3390/molecules24213892.

Theleritis C, Politis A, Siarkos K, Lyketsos CG. A review of neuroimaging findings of apathy in Alzheimer's Disease. Int Psychogeriatr 2014;26:195–207. https://doi.org/10.1017/S1041610213001725.

Tokimura H, Di Lazzaro V, Tokimura Y, Oliviero A, Profice P, Insola A, et al. Short latency inhibition of human hand motor cortex by somatosensory input from the hand. J Physiol 2000;523 Pt 2:503–13. https://doi.org/10.1111/j.1469-7793.2000.t01-1-00503.x.

Tombaugh TN, McIntyre NJ. The mini-mental state examination: a comprehensive review. J Am Geriatr Soc 1992;40:922–35. https://doi.org/10.1111/j.1532-5415.1992.tb01992.x.

Tuli HS, Tuorkey MJ, Thakral F, Sak K, Kumar M, Sharma AK, et al. Molecular Mechanisms of Action of Genistein in Cancer: Recent Advances. Front Pharmacol 2019;10:1336. https://doi.org/10.3389/fphar.2019.01336.

Udo N, Hashimoto N, Toyonaga T, Isoyama T, Oyanagi Y, Narita H, et al. Apathy in Alzheimer's Disease Correlates with the Dopamine Transporter Level in the Caudate Nuclei. Dement Geriatr Cogn Dis Extra 2020;10:86–93. https://doi.org/10.1159/000509278.

Uhlhaas PJ, Singer W. Abnormal neural oscillations and synchrony in schizophrenia. Nat Rev Neurosci 2010;11:100–13. https://doi.org/10.1038/nrn2774.

Vorobyov V, Bakharev B, Medvinskaya N, Nesterova I, Samokhin A, Deev A, et al. Loss of Midbrain Dopamine Neurons and Altered Apomorphine EEG Effects in the 5xFAD Mouse Model of Alzheimer's Disease. J Alzheimers Dis 2019;70:241–56. https://doi.org/10.3233/JAD-181246.

Vos SJ, Xiong C, Visser PJ, Jasielec MS, Hassenstab J, Grant EA, et al. Preclinical Alzheimer's disease and its outcome: a longitudinal cohort study. Lancet Neurol 2013;12:957–65. https://doi.org/10.1016/S1474-4422(13)70194-7.

Wechsler D. A standardized memory scale for clinical use. The Journal of Psychology: Interdisciplinary and Applied 1945;19:87–95. https://doi.org/10.1080/00223980.1945.9917223.

Wong DF, Rosenberg PB, Zhou Y, Kumar A, Raymont V, Ravert HT, et al. In Vivo Imaging of Amyloid Deposition in Alzheimer's Disease using the Novel Radioligand [18F]AV-45 (Florbetapir F 18). J Nucl Med 2010;51:913–20. https://doi.org/10.2967/jnumed.109.069088.

Zhao Q-F, Tan Lan, Wang H-F, Jiang T, Tan M-S, Tan Lin, et al. The prevalence of neuropsychiatric symptoms in Alzheimer's disease: Systematic review and meta-analysis. Journal of Affective Disorders 2016;190:264–71. https://doi.org/10.1016/j.jad.2015.09.069.